Norwegian University
of Life Sciences

**Master's Thesis 2023 30 ECTS**
Faculty of Science and Technology

# Batteries and supercapacitors – an equivalent circuit comparative study

Batterier og superkapasitorer –

en komparativ studie med ekvivalente kretser

Nicholas Ivar Willoughby
Environmental physics and renewable energy

# Preface

This thesis concludes my time as a student at the Norwegian University of Life sciences (NMBU). I wrote this thesis in the spring semester of 2023 as my final specialization in Energy physics in the Environmental physics and Renewable energy programme. The topics chosen in this thesis are interesting, and I would recommend other majors exploring them further from their respective points of view.

I chose batteries and supercapacitors as a subject due to the relevance of the topic in today's society with regards to sustainability, while I also wanted to learn more about supercapacitors. Both technologies chosen here have seen a wide use in different applications and are expected to expand their use further in future energy systems.

I would like to thank my supervisor Professor Dr. Jorge Mario Marchetti for all his input and his help with writing this thesis. Meeting once a week for individual feedback helped me immensely and was a good motivation throughout the semester. The monthly meetings with other master students also helped tremendously during the process of writing this thesis. I would also like to thank my mother, Kari Willoughby, for proof reading and general feedback on my thesis. Lastly, I would like to thank all the people I have met during my years of studying, especially my fellow students and lecturers in the courses I have taken over the last two years at NMBU.

Norwegian University of Life Sciences

Ås, 15. May 2023

Nicholas Ivar Willoughby

# Abstract

Using more renewable power is necessary to reach the sustainability goals set by the United Nations and reducing greenhouse gas emissions. Increased use of renewable energy is also required as many different sectors need to be electrified. Furthermore, the war in Ukraine has shown that relying on a foreign state's energy supply to guarantee enough power is not a viable strategy, and that more locally produced energy is needed. In order to achieve these ambitions, it is necessary to be able to store energy. Subsequently, both efficient supercapacitors and batteries are needed.

In this thesis a review of batteries and supercapacitors were carried out. First a short literature review was performed to see where batteries and supercapacitors are being used and how they perform. A second literature study was performed to study the modelling of batteries and supercapacitors. Equivalent circuit models for both batteries and supercapacitors were made. Two different batteries and supercapacitors were chosen for simulations. The batteries simulated were based on lithium ion and NiMH technology. The supercapacitors were chosen from two popular brands; Nichion and Eaton. The parameters for the different devices were decided by assuming that they behaved the same way as found in other studies in the literature. The devices were then simulated using a resistive load for a discharge cycle. Long-range simulations using CC-CV profiles were used.

Simulations showed that batteries were able to provide a charge for a longer time compared to the supercapacitors during discharging on a resistive load. During the CC-CV long-range simulation the Eaton 400F supercapacitor had the highest power output. Both supercapacitors were able to accomplish more cycles than both the batteries. The NiMH was able to do ½ cycle more than the lithium battery. The SOH calculations showed that the Nichion supercapacitor was able to achieve the most cycles. The lithium battery was able to perform more cycles than the NiMH battery.

# Sammendrag

Verden trenger mer fornybar kraft for å nå bærekraftsmålene satt av FN og redusere utslipp av klimagasser. Økt bruk av fornybar kraft er også nødvendig idet flere ulike sektorer skal elektrifiseres. Krigen i Ukraina har vist at det er sårbart å være avhengig av kraftproduksjonen i en fremmed stat, og at det er hensiktsmessig å produsere mer kraft lokalt. For å kunne nå disse målene er de nødvendig å kunne lagre energi. Følgelig er det behov for effektive batterier og superkapasitorer.

Denne masteroppgaven har sammenlignet batterier og superkapasitorer. Først ble en litteraturstudie gjennomført for å se hvor de respektive teknologiene blir brukt og hvor effektive de er. Etter dette ble en ny litteraturstudie gjort for å se hvordan man kunne lage gode modeller av begge teknologiene. Ekvivalente kretsmodeller ble deretter konstruert for både batteriene og superkapasitorene. To forskjellige batterier og superkapasitorer ble valgt for videre simuleringer. Lithium og NiMH batterier ble valgt som batterier. To aluminium superkapasitorer fra Eaton og Nichion ble valgt for superkapasitorene. Modellparameterne ble så etablert ved å anta at de forskjellige batteriene og superkapasitorene hadde like parametere som var funnet i litteraturen.  superkapasitorene og batteriene ble deretter simulert ved å bruke en resitiv last for en utladningssyklus.  Etter dette ble batteriene og superkapasitorene simulert ved å bruke en CC-CV metode over flere sykluser.

Simuleringene viste at batteriene kunne gi en effekt over lenger tid sammenlignet med superkapasitorene. Under CC-CV over flere sykluser ga Eaton 400F superkapasitoren den høyeste effekten.  Begge superkapasitorene kunne brukes over flere sykluser enn batteriene kunne ved bruk av en CC-CV metode. NiMH batteriet klarte å gi ½ ekstra syklus sammenlignet med Lithium batteriet ved samme tidsperspektiv. SOH-simulasjonen viste at Nichion superkapasitoren kunne levere flest sykluser før den nådde sitt sluttpunkt.  For batteriene hadde Lithium batteriet lengst levetid når man så på faktiske antall sykluser.

# Table of content

# List of figures

# List of tables

# List of equations

# 1. Introduction

## 1.1 Background

The United Nations sustainability goal number 13 is to stop climate change [1]. To achieve this goal the world needs to phase out fossil fuels and non-renewable sources [2]. This has been embodied in the Paris agreement where 196 countries have agreed to reduce their greenhouse gas emissions by 43% by 2030 [3]. Increasing renewable production is needed in order to reach this goal.

To incorporate the influx of renewable energy the need to be able to store it efficiently arises. At the same time renewable energy alone cannot meet the grids required power output during peak demands [4]. There are multiple industries in Norway that rely on fossil fuels. These are primarily the transportation sector, the offshore sector, and power intensive land-based industry [5]. The Norwegian Water Resources and Energy Directorate estimates that to electrify these three sectors the Norwegian energy demand would increase by 23 TWh [5]. To be able to reach this goal using renewables as the main source, batteries and supercapacitors are required [4].

The war in Ukraine has shown that relying on a foreign state's energy supply to guarantee enough power is not a viable strategy. This has highlighted the importance of being able to produce and store energy as close to the consumer as possible. As renewable energy can be produced anywhere in the world, a country can in theory produce enough energy to cover its own need within its own border. In May 2022 the European Commission released a plan to phase out Russian natural gas from its energy mix [2]. The objective of the plan is to increase the amount of renewable energy in the grid as well as build an energy infrastructure that is not connected to Russia [2]. To achieve this the European Union needs to save energy, diversify its energy mix, and build more renewable energy power plants. In regard to increasing the number of renewable sources in the energy mix the EU plans to phase in more solar and wind power [2].

Solar and wind power only produce energy when the weather allows it. For the grid this might mean that the power being produced will vary based on the local weather. This can cause a problem where there will be a mismatch between production and consumption [6].

To mitigate some of these issues and to phase out fossil fuels energy storage is needed [4]. There are many different types of energy storages such as batteries, supercapacitors and pumped hydro. This thesis will focus on batteries and supercapacitors. Supercapacitors and batteries can be found in different industrial sectors. In the grid, batteries and supercapacitors can help store excess energy [4] [6]. In the transport sector the main electrification will implemented by replacing fossil powered car with electric vehicles running on batteries [5]. In the offshore sector, batteries and supercapacitors are some of the different types of energy storages that can help incorporating technologies like offshore wind.

## 1.2 Objectives/Scope

The objective of this thesis is to compare supercapacitors with batteries in order to determine where each of the different energy storages excel and to identify the main issues with different applications. To answer this, a literature study of batteries and supercapacitors will be carried out to see the strengths of the different types of energy storage devices, and the weaknesses that needs to be investigated and improved on further. Equivalent circuit models of batteries and supercapacitors will be made to study their performance and their estimated State of Health (SOH). All these aspects will help determine possible areas of use for batteries and supercapacitors and the different strengths and weaknesses of the two technologies.

# 2. Theory

## 2.1 Batteries

### 2.1.1 General

Batteries are electrochemical devices that store energy within their chemical compound [7]. There are two different types of batteries; primary and secondary batteries. The main difference between these is that a primary battery can only be used once and is not rechargeable [7]. A secondary battery can be discharged and charged multiple times [7].

### 2.1.2 Redox reactions

When using batteries electricity needs to be stored as chemical energy in order to be able to transform back to electricity when the electricity is needed.

A redox reaction is a reaction that transfers electrons between two different mediums [8]. The redox reaction can be split into two different half reactions. During a reaction, the anode is oxidised and the cathode is reduced. Which electrode is the anode or the cathode depends on whether the battery is being charged or discharged. The general form for the half reactions for the negative electrode is given in Equation 1. The positive electrode is given in Equation 2.

$$A \rightarrow A^{n+} + ne^{-}$$

Equation 1: Half reaction at the negative electrode [7]

A is a metal, n is the number of charges being transferred in the process.

$$nB + ne^{-} \rightarrow nB^{-}$$

Equation 2: Half reaction at the positive electrode [7]

B is a metal oxide and $e^{-}$ is the electrons being released in the process.

During the discharging of the battery, the electrons move from the anode to the cathode. The current, however, moves in the opposite direction of the electrons. The anode will be the negative electrode and the cathode will be the positive electrode. When the battery is being charged, the anode and the cathode switch places. Each half reaction will have an electric potential [7]. The total reversible voltage that a cell can deliver is described in Equation 3.

$$E_{cell}^{0} = E_{red}^{0} + E_{oks}^{0}$$

Equation 3: Reversible cell voltage [8]

$E_{cell}^{0}$ is the reversible cell voltage, $E_{red}^{0}$ is the reversible reduction potential and $E_{oks}^{0}$ is the oxidation potential

### 2.1.3 Thermodynamical theory

There are different ways to quantify the different functions of states that are present in electrochemical reactions for batteries. The different ways of explaining these states in a chemical system can be divided into internal energy, enthalpy, entropy and Gibbs free energy [9].

The internal energy of a thermodynamic system is defined as the sum of kinetic and potential energy within the system [10].

For a reversible system with no change of volume the change of enthalpy can be defined as the amount of heat in the system [11]. The definition of the change of enthalpy for a reaction is given in Equation *4*.

$$\Delta H = \Delta U + P\Delta V$$

Equation 4: The change of enthalpy for a reaction *[10]*

$\Delta H$ is the change of enthalpy, $\Delta U$ is the change of internal energy and $P\Delta V$ is the pressure times the change of volume.

There will always be energy within a chemical compound that cannot be converted to useful work in a reaction [11]. To explain this loss of energy entropy must be defined. Entropy can be defined as the amount of thermal energy that cannot be used for useful work divided by the temperature in the compound [8] [10]. As molecules need to move in an ordered way to perform work, entropy can also be viewed as the amount of randomness in a system [10].

To be able to use the stored energy in a battery it is preferable that the reaction is spontaneous. This means that extra external energy does not need to be added for the reaction to happen. For a fully charged battery this means that the electrons in the battery should move and transfer energy as soon as the reaction takes place [10]. On a reaction level

Gibbs free energy states whether a reaction is spontaneous [10]. In terms of work the change of Gibbs free energy can describe how much work a thermodynamical system can perform [8]. The change of Gibbs free energy is defined in Equation *5*.

$$\Delta G = \Delta H - T\Delta S$$

Equation 5: Change in Gibbs free energy for a chemical reaction *[10]*

*$\Delta G$ is the change in Gibbs free energy, $\Delta H$ is the change in enthalpy, T is the temperature in kelvin, $\Delta S$ is the change in entropy*

The change in Gibbs free energy can also be calculated based on the total cell potential or the reversible cell voltage. As the change in Gibbs free energy describes the total work a chemical system can perform, it can be related to the cell potential and is shown in Equation 6 [12]. It is important to note that the equation is valid for both the total cell potential and the reversible cell potential. Which potential that is chosen, defines whether you get the total change of Gibbs free energy or the reversible change in Gibbs free energy.

$$\Delta G = -nFE$$

*Equation 6: Gibbs free energy in terms of cell potential [12]*

n is the number of electrons transferred in the reaction, F is the Faraday constant and E is the cell potential

### 2.1.4 The Nernst equation

Batteries usually perform under non-standard and non-ideal conditions [11]. To help describe the cell potential the equilibrium constant must also be taken into consideration. The equilibrium constant describes the ratio between reactants in an electrochemical reaction [8]. For a total chemical reaction given in Equation *7*, the equilibrium constant can then be shown in Equation 8.

$$aA + bB \rightleftharpoons cC + dD$$

Equation 7: Overall electrochemical reaction *[11]*

*a,b,c,d is stochiometric numbers, and A,B,C,D are reactants*

$$K = \frac{[C]^c[D]^d}{[A]^a[B]^b}$$

Equation 8: The equilibrium constant [11]

C,D,A,B are given in the unit molar(M).

The equilibrium constant can then be used to calculate more accurately the total cell potential that can be achieved in an electrochemical reaction [8]. This leads to the Nernst equation which is used under non-standard conditions. Using the definitions from Equation 6, Equation 3 and Equation 8 the Nernst equation can be derived as shown in Equation 9 [12].

$$E = E^0 - \frac{RT}{nF}\ln(K)$$

Equation 9: The Nernst equation [12]

E is the total cell potential, $E^0$ is the standard reversible cell potential, R is the universal gas constant, n is the number of electrons transferred and F is the Faraday constant.

### 2.1.5 Electrodes and electrolyte

In the anode electrons are being released to the external circuit that is activated during charge/discharge [7]. The cathode catches the electrons during the reaction and releases a current that can be used during discharge [7]. The materials being used in the electrodes are primarily metals and metal oxides [12]. For the batteries to be as efficient as possible the electrodes have to have certain characteristics. The anode has to have properties which ensure it can be reduced efficiently and is stable in contact with the electrolyte [7] [12].

In a battery the role of the electrolyte is to make the ions able to move between the electrodes [7]. The electrolyte that can be used have different states of matter depending on the battery chemistry and electrode materials. These states are mainly aqueous and solid [12].

For lithium secondary batteries it is also important that the electrolyte has properties that allow lithium ions to be exchanged on the surface of the lithium electrodes [12]. In general, the electrolyte also has to be a poor electrical conductor and not react with the electrodes [7]. This is necessary to avoid short circuiting the battery and make sure that electrons and ions do not move through the external circuit that the battery is connected to. In Figure 1 a schematic of a lithium battery is shown. Here the anode, cathode and the electrolyte are shown. It also shows where the electrons and ions move during charging and discharging.

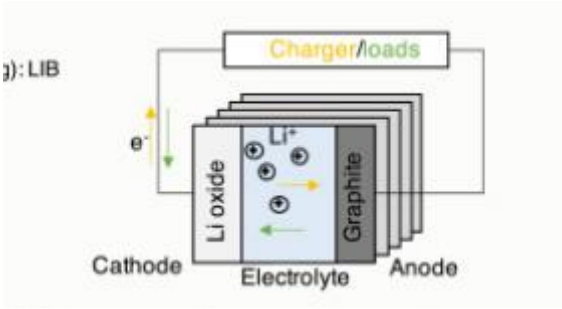


*Figure 1: Schematic of a battery with Anode, Cathode and Electrolyte. Given under a creative commons license (CC-BY-NC 4.0) Reprinted from: [13]*

### 2.1.6 Capacity, energy density and power for batteries

Capacity, energy density and the power that the battery can supply is important for different applications. The capacity of a battery is the amount of charge a battery can deliver under certain conditions. The unit is given in Ah [12]. The theoretical capacity of a battery can be calculated using Equation 10.

$$C_T = nF$$

Equation 10: Theoretical capacity [12]

n is the number of electrons released in the process and F is the faraday constant.

As batteries are being used in a wide range of applications a way of calculating how long the battery can be used, and how long it will take to charge the battery is needed [7]. This can be done by looking at the C-rate for the specific energy storage device. The C-rate denotes the time a battery needs to be charged or how long it can be discharged during different currents [12] [7]. The time required for charging and discharging can be calculated with Equation 11.

$$t = \frac{C}{i}$$

Equation 11: Charge and discharge rate [12]

t is the time in hours, C is the capacity and i is the current

The energy density of an energy storage device is defined as how much energy that can be stored per units of volume or mass [7]. The unit for energy density is given as Wh/kg, Wh/l. The energy density of a battery can be calculated using Equation 12 and Equation 13.

$$E_\rho = \frac{C_{ah} \cdot E}{m}$$

Equation 12: Energy density (Wh/kg) *[7]*

$$E_\rho = \frac{C_{ah} \cdot E}{V}$$

Equation 13: Energy density (Wh/m3) *[7]*

$C_{ah}$ is the capacity of the battery, E is the voltage, m is the mass of the battery and V is the volume of the battery.

The power a battery can deliver is defined as the energy the battery gives over a time t [7] [12]. The power can be calculated using this relationship and is shown in Equation 14.

$$P = i \cdot E$$

Equation 14: Power equation *[12]*

P is the power output, i is the current and E is the voltage of the battery

### 2.1.7 Losses

The open circuit voltage is the best-case scenario for the voltage that can be delivered by the battery. There are three main losses for battery systems that limit the total voltage that the battery can deliver [7]. These are ohmic losses, activation losses and concentration losses [12].

Ohmic resistance happens due to electrons moving through the electric circuit, as well as ions moving through the electrolyte and the membrane of the battery [14]. The activation energy is energy that that is required for a reaction to happen [8]. The activation energy is shown in Figure 2.

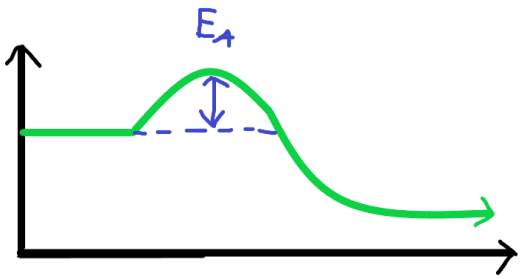


Figure 2: Activation energy for a chemical reaction *[11]*

The concentration losses are related to the moving of ions during charging and discharging. This can be shown using Equation 9, as well as Equation 8. As the equilibrium constant is changing during a reaction the equilibrium constant can either favour reactants, products or be in equilibrium.

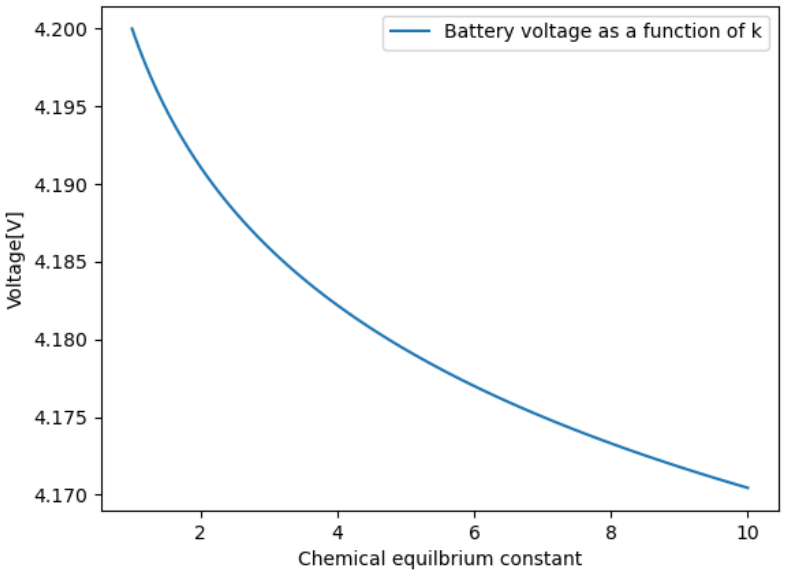


*Figure 3: Voltage as a function of K*

Figure 2 shows that the voltage is being reduced as K is increasing. The plot in figure 2 is based on Equation 9 with a constant voltage of 4.2 V to show the voltage with a varying K.

Due to these loss mechanisms the total voltage that the battery can deliver can be calculated using Equation 15. During charging the battery needs to be given more voltage to overcome these losses [7]. The total voltage required to charge the battery will be the open circuit voltage, in addition to the voltage required to combat the other loss mechanisms [12].

$$E_d = E_{ocv} - \eta_+ - \eta_- - IR - \eta_{act} - \eta_{conc}$$

*Equation 15: Actual voltage [7]*

Ed is the actual voltage, $E_{ocv}$ is the open circuit voltage, $\eta_+ - \eta_-$ are the overpotentials at the positive and negative electrodes, $\eta_{act}$, is the activation losses, $\eta_{conc}$ is the concentration losses and IR is the ohmic losses.

## 2.2 Supercapacitors

### 2.2.1 General

Supercapacitors are energy storage devices that store energy within an electrochemical double layer at the electrodes [15]. In the double layer there is an electric field, which is where the energy is stored. Positive and negative charges in the electrolyte accumulate to compensate for the electric charge on the surface of the electrodes [15]. This creates an electric field that will conserve the charge in the capacitor, even if a current is removed [16]. A supercapacitor is divided into the electrodes and a dielectric medium, where an electrolyte is being used. The electrodes are separated by an electrolyte as well as a separator [15].

### 2.2.2 Capacitance

Capacitance is how much charge can be stored at a given voltage in a capacitator [16]. The capacitance C for a capacitor is defined as "the ratio of the magnitude of the charge on one of the plates to the potential difference between them" [16]. The capacitance is given in Equation 16.

$$C = \frac{Q}{V}$$

*Equation 16: Capacitance [16]*

C is the capacitance; Q is the charge and V is the voltage.

### 2.2.3 Conductance and inductance

Conductance is the measure of how well current can flow through a material. The inductance is the measure of how an inductor can resist a change in current that flows through it [16].

### 2.2.4 Electrodes and electrolyte for supercapacitors

Supercapacitors can use a wide range of different electrode materials as well as different types of electrolytes [15]. Carbon is the most used electrode material for supercapacitors [16]. This is mainly due to carbon having a wide surface area, being less expensive than other options and because carbon is a material that is easy to manufacture [15].

The second type of material that can be used as materials for the electrodes are metal oxides [17]. The metal oxides that can be used are RuO2 and IrO2 amongst others [15]. These materials have a high production cost and are only usable with an aqueous electrolyte [17].

The third type of electrode material that are used for supercapacitors are polymers [15]. Polymers for usage in supercapacitors are materials that are made from n and p-doping of different materials to form long chains of small structures [15] [11]. The polymer supercapacitors can give a high specific power output, but are not stable enough to run for a long time [15]. In Figure 4 the schematic for a general supercapacitor is shown. It shows where the positive and negative charges are stored, and where the electrons and ions travel during charging and discharging.

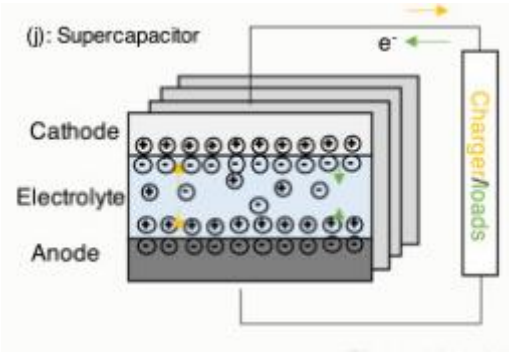


*Figure 4: General schematic for supercapacitors. Given under a creative commons license (CC-BY-NC 4.0) Reprinted from: [13]*

Table 1 gives an estimate of what order of magnitude the specific capacitance can be for different types of electrode material as well as the maximum voltage.

Table 1: Specific capacitance for different supercapacitors

| Material family | Electrode | Specific capacitance | Electrolyte | Voltage(max) |
|---|---|---|---|---|
| Carbon-based | Nitrogen-porous doped carbons (NPC) | 98.70 F/g [18] | KOH (alkaline solution) | 1.23 V [19] |
| Metal oxides | $Co_3O_4$ | 201.3 F/g [20] | Na2SO4 (aqueous) | 1 V [19] |
| Polymer | Polyaniline | 298 F/g [21] | Al(NO3)3 | 2.7 V [15] |

### 2.2.5 Capacity, energy density and power for supercapacitors

The capacity, energy density and power density are important to know for supercapacitors as well. The energy that a supercapacitor can store is proportional to the capacitance of the electrodes as well as the voltage the capacitor is rated for [15]. Equation 17 defines the maximum energy a supercapacitor can store.

$$E_{s.c} = \frac{1}{2} C V^2$$

*Equation 17: Energy stored in a supercapacitor [4] [15]*

C is the capacitance, and V is the voltage

The capacity of a supercapacitor depends on many different variables such as discharge time, discharge current and general load/charging profiles. For a supercapacitor the total capacity can be estimated using Equation 18.

$$C_{s.c} = \frac{C \Delta V}{3600}$$

*Equation 18: Capacity estimation of a supercapacitor [22]*

$C_{s.c}$ is the Capacity of the supercapacitor, C is the capacitance of the supercapacitor and $\Delta V$ is the voltage change from the OCV to the cut-off voltage.

The power a supercapacitor can deliver is based on the voltage as well as the series resistance [4] [15]. In Equation 19 the power that a supercapacitor can provide is defined.

$$P = \frac{V^2}{4R}$$

*Equation 19: The power output from a supercapacitor [15]*

V is the rated voltage, and R is the series resistance

The energy density, specific capacity and power density follow the same principles as presented in the section for batteries. If these quantities are used later in the thesis the author has used the equations above and divided by mass or volume depending on what parameter is needed.

### 2.2.6 Electrical foundation

Both batteries and supercapacitors contain electrical and chemical elements that work together to deliver the desired output. Some of the electrical equations that provide insight into the electrical elements that are present in battery and supercapacitor models will be presented here.

Electrical components can be either linear or non-linear depending on their properties or behaviour during electrical operations. Capacitors and inductors can both be described using linear differential equations [16].

The current through a linear capacitor is defined as the capacitance times the change of voltage over time. This is shown in Equation 20.

$$I = C\frac{dV}{dt}$$

*Equation 20: The current through a linear capacitor [16]*

I is the current, C is the capacitance and dV/dt is the change of voltage over time.

The voltage flowing through an inductor can be described as the inductance times the change of current over time. This is shown in Equation 21.

$$V = L\frac{dI}{dt}$$

*Equation 21: The voltage through an inductor [16]*

V is the voltage; L is the inductance and dI/dt is the change of current over time.

## 2.3 State of charge and state of health

The state of charge (SOC) and state of health (SOH) is important to know for both batteries and supercapacitors. The SOC and SOH in the literature have many different definitions based on the applications where the energy storage device is being used and what parameters are known, as well as how fast the SOC and SOH need to be calculated. The speed required for SOC/SOH depends on what kind of battery management system(BMS) that is being utilized [23]. For example, a SOC calculation for an electric vehicle needs to be fast to avoid suddenly running out of charge while still driving, whereas in a BMS it is important to know the SOH for better prediction of the SOC over time [4]. However, the SOH is not a factor the system needs to know from cycle to cycle.

There are many different types of methods to calculate the SOC, including Kalman filtering and coulomb counting [24]. Coulomb counting has both positive and negative traits when applied. For the case of this thesis the coulomb counting method is fast and sufficiently enough to be applied. Coulomb counting is defined in Equation 22 below.

$$SOC(t) = SOC(t_0) - \int_0^t \frac{I(t)}{C_{bat}} dt$$

*Equation 22: SOC calculations using coulomb counting [24]*

$SOC(t)$ is the state of charge at point t, $SOC(t_0)$ is the initial state of charge, and $\int_0^t \frac{I(t)}{C_{bat}} dt$ is the integration of the current flowing through the battery over time t.

The state of charge varies based on the current drawn and the initial SOC. Figure 5 below shows how the SOC may vary for a battery during discharging with a resistive load.

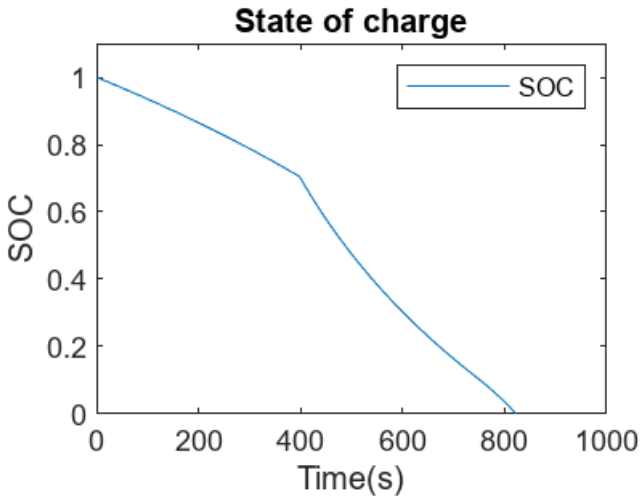


*Figure 5: SOC(t) for a battery during discharging*

During charging the SOC(t) will increase until the SOC reaches 1, depending on how aging is modelled. The change of slope seen in Figure 5 occurs due to the different polarization in the storage device. The current, I(t) was here increasing over time. The voltage over time was decreasing until the SOC(t=802s) reached 0.

For supercapacitors there are many ways of calculating the SOC. Some of these are Kalman-filtering, an ampere hour approach and max energy approach. As there are many different benefits and limitations to all the different ways of calculating the SOC, this thesis will use the max-energy approach when calculating the SOC for supercapacitors [25]. Here the SOC is calculated using the energy that the supercapacitor is providing, divided in relation to the energy the supercapacitor is rated for. By using Equation 17 on page 21 the SOC can be defined as shown in Equation 23 below.

$$SOC_{S.C} = \frac{V_{load}^2}{V_{rated}^2} 100\%$$

*Equation 23: SOC for supercapacitors using the energy method [25]*

For a supercapacitor the SOC(t) calculated by using the energy method is shown in Figure 6.

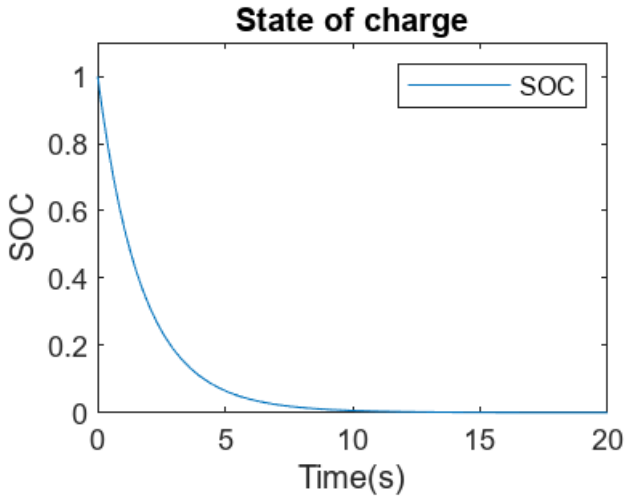


*Figure 6: SOC for a supercapacitor connected to a resistive load*

For both supercapacitors and batteries, the SOH can be defined based on the capacity degradation over time [26]. As the energy storage device is charged and discharged over time, the maximum capacity that can be stored will decrease. Equation 24 shows one method that can be used to calculate the SOH.

$$SOH(n) = \frac{C_{max}(n)}{C_{rated}} 100\%$$

*Equation 24: SOH over time [26]*

SOH(n) is the SOH over cycles, $C_{max}(n)$ denotes the energy storage devices ability to store energy over multiple cycles. C rated is the rated capacity of the energy storage device

The SOH for a battery will degrade over multiple cycles. There are many different factors that play a part in the degradation of batteries. Some of them are aging, temperature, charging/discharging over time, increased resistance and corrosion that reduce the available area for ions to move [7] [9] [17].

## 2.4 Literature review

The aim of the literature review was to see where and how supercapacitors and batteries are being used, and also to highlight some of their advantages and disadvantages within the applications.

Durganjali et al. [4] investigated using batteries and supercapacitors in grids with a large share of renewables like solar and wind. The main areas where batteries and supercapacitors can support the grid are voltage regulation and power feeding. The major issue that batteries and supercapacitors cause in the grid is a higher cost of electricity. The high cost of electricity due to lithium batteries was found to be caused by slow charging time [4]. For the supercapacitor the rapid charging and discharging meant that the supercapacitor alone in the grid could not provide a sufficiently stable charge over time. Durganjali et al. [4] then combined supercapacitors with lithium-ion batteries to reduce the cost of electricity. By doing this, the authors achieved a cost of electricity of about 0.32$/kwh, compared to 0.33$/kwh for a normal lithium battery.

Powade et al. [27] studied the use of batteries and supercapacitors together and as standalone units. By using lithium batteries alone, the authors observed that the battery system was more prone to degradation and that the general size required for the battery system was quite large in terms of the power required. This increased the cost, weight, and volume of the system [27]. By using real world driving data, the authors showed that a standalone battery could handle about 2442 cycles before reaching a SOH of 80% [27]. When combining the supercapacitor with the battery system the estimated number of cycles were 2660 [27].

Supercapacitor buses were used in the 2010 World Expo in Shanghai [28]. The buses only had enough charge for one trip and needed charging after every trip [29]. As the supercapacitors have a short charging time, the buses were fully charged after a couple of minutes [29]. By doing this the busses at the Expo achieved an uptime of about 100% [28] [29]. Some of the disadvantages of the supercapacitors were noted by Guo et al. [28]. These included having a high self-discharge rate, high cost, low power density when compared to a lithium-ion system with the same rated energy as the supercapacitor [28].

# 3 Methodology

## 3.1 Models available for energy storage devices

Many different types of models of batteries and supercapacitors are found both in the literature as well in actual applications. Battery and supercapacitor models might be used in battery management systems (BMS), or they might be used to simulate performances for specific energy storage devices. The objective for required output of the model decides the level of complexity necessary in the model.

The different models require different types of input depending on the output that is sought from the model. Some of these models will be presented here.

The most complex models are physical models where one makes partial differential equations for a battery or supercapacitor based on their electrochemical layout. These models capture most of the physical properties a supercapacitor or battery has [24]. These models, however, have a long run time, and often require a lot of computing power compared to other models that are available [30]. Doyle, Fuller and Newman have developed models for Li-ion batteries by coupling 6 non-linear differential equations [31]. Petit et al. [30] proposed a simplified version of these models which required less computational power, but was not as accurate as the Newman model [30].

Thermal models are made to study the thermal performance of batteries and supercapacitors, whilst also looking at how thermal effects influence the performance. These models can either be run on their own or be coupled with electrochemical models based on what factors might affect the model [32]. Thermal models are useful as heat generation within energy storage cells varies depending on load, as well as the environment they are in [32]. Since heat generation also influences aging and capacity fade, these models can be useful for calculating the SOH [32] [14].

Equivalent circuits are also a type of model that might be used for batteries and supercapacitors. These models can be as complex as required for different applications. Depending on what energy storage technology is being used, they can capture a wide range of the different dynamics of a storage system. Equivalent circuit models require less computational power when compared to electrochemical models [4]. The main issue for these

models is finding parameters for the different branches in the circuit, while also capturing the long-term behaviour of the energy storage device [4] [31]. Each battery and supercapacitor cell will have different parameters in the resistor-capacitor (RC) branches. These models have become more accurate over the years, but at the same time also lack verification without lookup tables which are gained from experimental data [31].

In this thesis equivalent circuit models were chosen for both supercapacitors and batteries in terms of building a simulation basis. Equivalent circuit models were chosen due to the wide selection of pulse tests that have been carried out for many different storage chemistries in the literature. Equivalent circuits were chosen as simulated performance provide a good indication as to how the different storage technology behaves. Two types of simulations were decided to be performed. One simulated the long-term behaviour, and the other simulated the performance when connected to a resistive load for one full discharge cycle.

## 3.2 Deriving a model for batteries

Different types of battery cells have different charging and discharging characteristics. Due to time constraints equivalent circuit models for batteries were chosen in this thesis. Equivalent circuit models for batteries provides an explanation for most of the different battery behaviour. This provides a simple way to set up a simulation that can be used to compare different battery chemistries [33]. In Nikhil et al. [34] an equivalent circuit model was made to study Li-ion batteries when different currents were applied to the models. The objective was to create a battery model that could be used for BMS and used to control electrical vertical take-off and landing aircraft. To do this Nikhil et al. [34] made an equivalent circuit model that was able to capture most of the underlying physics, while also being computational efficient.

Stefan Skoog [35] studied equivalent circuit models for hybrid electric vehicles. Here three different equivalent circuits were studied with different levels of complexity. The first model was a basic circuit with an OCV terminal and 1 resistor in series. The second and third circuit models included 1 resistance in series and 1 RC branch for the 2nd model and 2 RC-branches for the 3rd model [35]. These models are shown in Figure 7 Figure 8 and Figure 9.

Stefan Skoog [35] then carried out pulse tests for different lithium batteries to measure the different resistances and capacitances. The difference between the voltage root mean square was decreased while using 2-RC branches rather than one for long load cycles [35]. The time constant for the first RC branch was set to about 10 seconds, while the time constant for the second RC branch was set to between 100-200 seconds [35]. For RC models the 2$^{nd}$ RC branch is often seen as the branch which takes long range dynamics into consideration as well as diffusion [34] [33] [35]. To obtain the correct parameters for equivalent circuits it is important that the OCV is measured accurately as this has an effect in pulse tests [35].

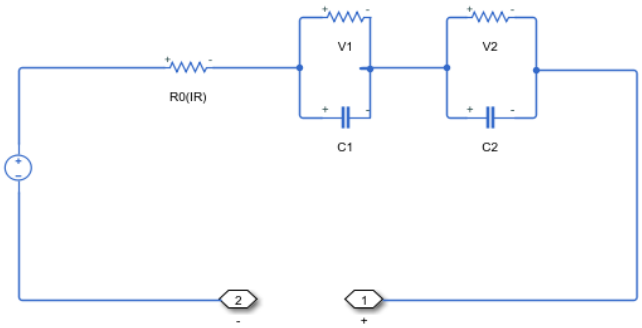


*Figure 7: Equivalent circuit model with 2 RC branches. Given under a creative commons license (CC-BY-NC-ND 4.0), Reprinted from: [36]*

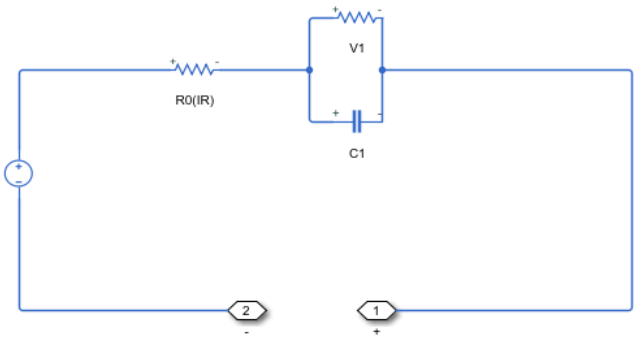


*Figure 8: Equivalent circuit model with 1 RC branch Given under a creative commons license (CC-BY-NC-ND 4.0), Reprinted from: [36]*

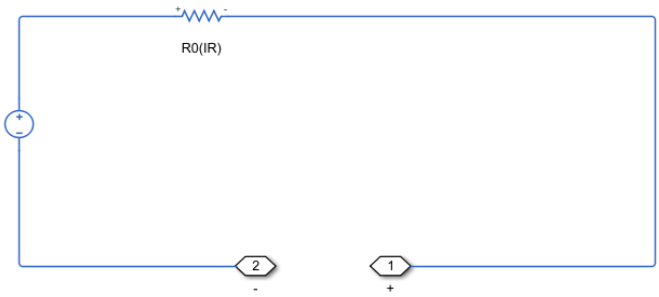


*Figure 9: Equivalent circuit model with only one resistance Given under a creative commons license (CC-BY-NC-ND 4.0), Reprinted from: [36]*

Fan et al. [37] presented some of the disadvantages and limitations that can be found in equivalent circuit models and proposed a non-linear equivalent circuit model to mitigate these limitations. As an electrochemical model(ECM) tries to explain the dynamics of the system rather than the physics behind the battery, a wide range of physical information cannot as easily be explained compared to mathematical/physical models [37]. This especially affects models which try to describe lithium-ion batteries, as the RC-branches used do not capture the long-term diffusion kinetics that is observed in lithium batteries [37]. This can often be observed as the time constant for the 1$^{st}$ RC branch as seen in Stefan Skoog [35] was set to 100-200 seconds. In order to capture some of the long-term behaviour of this diffusion, a non-linear model can be used, where the time constant is set to 1000 seconds [37]. The battery can then be modelled using non-linear capacitors and resistances. By doing this Fan et al. [37] obtained a more accurate model compared to a normal equivalent circuit model with a RMSE of 49.6 % when compared to each other [37].

In this thesis it was decided that an equivalent circuit model with 2-RC pairs would be used to simulate battery performance. This was done in order to capture some of the transient behaviour that batteries have, while also not having models that would be too complex and uncertain without any experimental data to validate the model. The models were then built in MATLAB Simulink with the simscape and simscape electrical addons. These equivalent circuits are often called second order Thevenin circuits as they share some of the properties that Thevenin circuits have in an electrical perspective [38]. However, the second order Thevenin-model does not consider factors like temperature and capacity [39].

By using Equation 22 and assuming that the voltage flowing through the circuit as a function of SOC; $f(SOC(t))$ and then assuming that the OCV is the same as the reversible cell potential as presented in Equation 3, this gives the voltage of the battery over time.

$$v(t) = E^0_{cell}\big(SOC(t)\big) - v_{C1}(t) - v_{C2}(t) - i(t)R_0$$

*Equation 25: Voltage through an equivalent circuit model [38] [33] [39]*

$v(t)$ is the voltage over time in the battery, $E^0_{cell}\big(SOC(t)\big)$ is the OCV as a function of SOC, $i(t)R_0$ is the current times internal resistance while $v_{C1}(t)$ and $v_{C2}(t)$ are the voltage dynamics in the RC branches

There are some simplifications that can be performed on Equation 25 depending on how many RC branches that are present in a model. If the model in question only has a resistance $v_{C1}(t)$, $v_{C2}(t)$ can be removed. If only one RC-branch is present, $v_{C2}(t)$ can also be removed [39].

$v_{C1}(t)$ and $v_{C2}(t)$ can be expressed in terms of voltage using Kirchhoff's circuit law [38] [40]. This was presented in [40] [41], and gives:

$$\frac{di_{Rn}}{dt} = -\frac{1}{R_n C_n} i_{Rn}(t) + \frac{1}{R_n C_n}$$

*Equation 26: Current through RC branches [41] [40]*

$\frac{di_{Rn}}{dt}$ is the time dependant current through rc-branch n, $R_n$ is the resistance in branch n, $C_n$ is the capacitance in branch n.

There are different ways to solve the equations that arise from the different models. The equations can be converted into discrete time, solved directly as a system of ODEs or be solved numerically. Simulink has a variety of tools to solve these equations which are based on implicit and explicit methods.

It is important to determine what the RC-parameters are for a specific battery. There are multiple ways that can be used to decide the different parameters. The most popular are electrochemical impedance spectroscopy (EIS) or pulse-discharge tests [42]. In this thesis no

experiments have been carried out. All the relevant RC-parameters have therefore been estimated based on EIS or pulse tests from the literature.

Two different batteries with different chemistries were chosen for further simulations. One Lithium ion (Li-ion) battery cell and one nickel metal hydrate (NiMH) cell were chosen. All the relevant information for the different cells is given in Table 2.

*Table 2: Chosen battery properties*

| Battery | BM2000C1450AA2S1PATP | ICR18650-26F |
|---|---|---|
| Chemical technology | NiMH | Li-ion(Cylindrical cell) |
| $I_{discharge}$ | Not provided in datasheet | 5.2 A |
| $I_{charge}$ | 1 A (0.5C) | 2.6 A |
| Capacity | 2 Ah | 2.6 Ah (0.2C) |
| $V_{max}$ | 1.32 V(max charging voltage) | 4.2 V |
| $V_{ocv}$ | 2.4 V | 3.7 V |
| $V_{cutoff}$ | 1 V | 2.75 V |
| Dimensions | 28.5*51.5*16.5 mm (l*w*h) | 18.4*65.00 mm (D*h) |
| Weight | 60.0 g | 47.0 g |

In order to simulate the behaviour of the batteries two different types of models were made in Simulink. One was made coupling the 2$^{nd}$ order equivalent circuit model with a resistive load to simulate the batteries during discharge. The circuit model is given in Figure 7. The load was made in Simulink using a varying resistor in combination with a constant inductor. The resistance for the resistor could then be manipulated by sending a signal to the resistor. The load block is shown in Figure 10. In Figure 11 the complete set up of the equivalent circuit with a resistive load is shown.

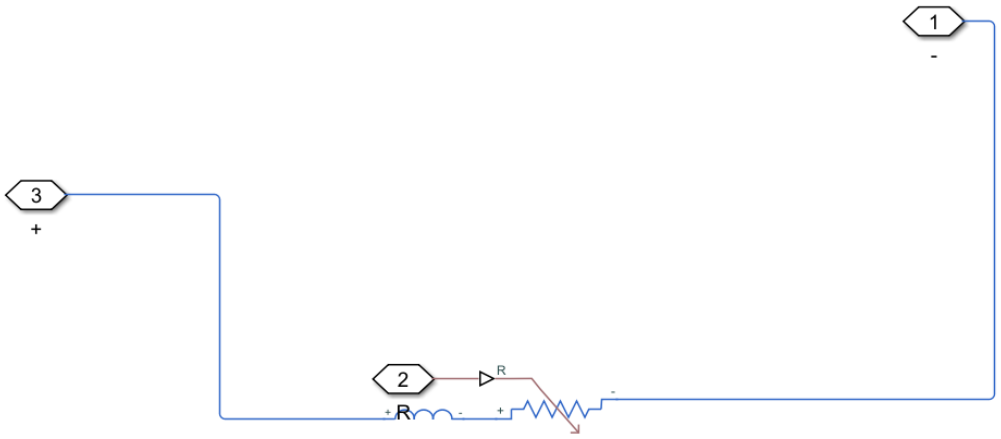


*Figure 10: The resistive load used in Simulink*

In Figure 10, 3 is the connection for the positive terminal, 1 is the connection for the negative terminal and 2 is the input for the resistance signal.

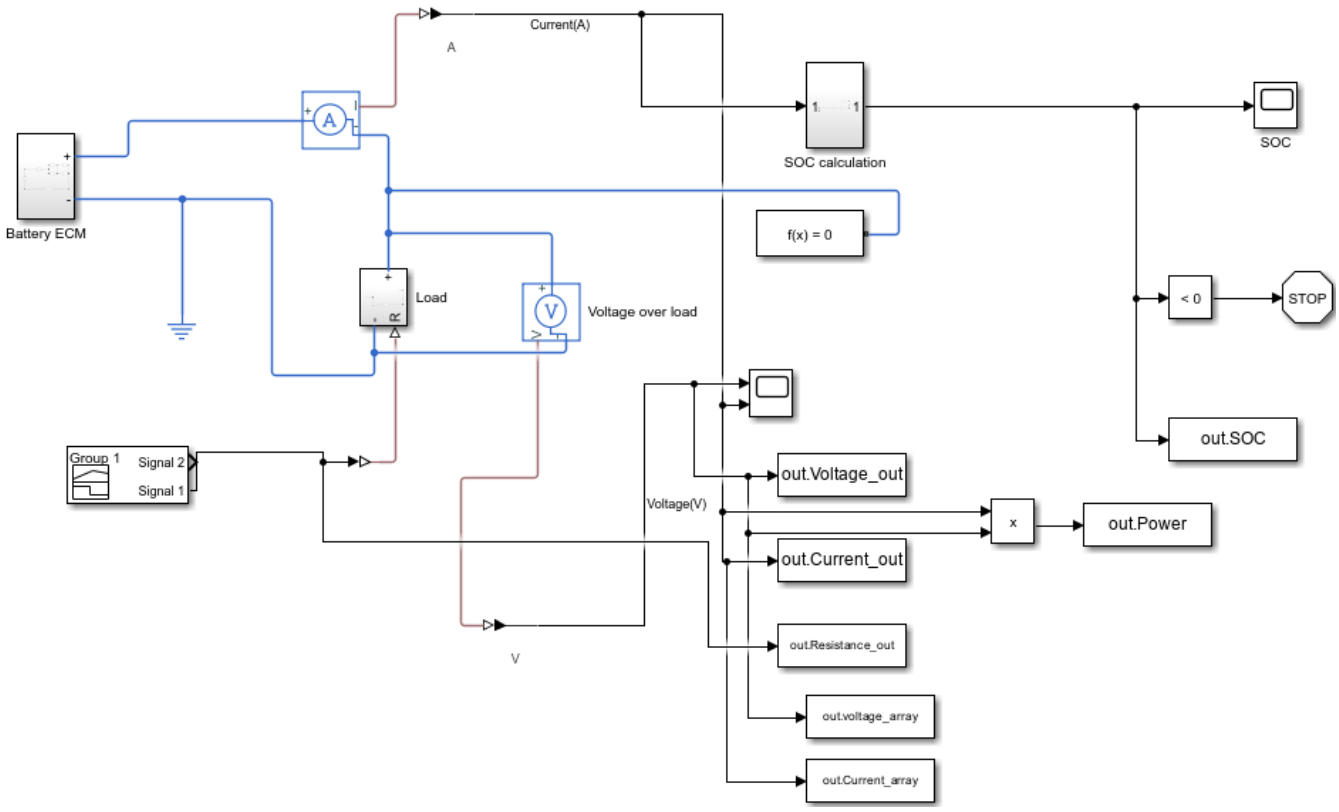


*Figure 11: Equivalent circuit model in Simulink with a resistive load*

Simulink combines the equations given in the theory section, makes a system of equations and solves them over time. The relevant equations Simulink uses are Equation 20,Equation 21, Equation 25 and Equation 26, these are shown below in the same order.

$$I = C\frac{dV}{dt}$$

$$V = L\frac{dI}{dt}$$

$$v(t) = E_{cell}^{0}\big(SOC(t)\big) - v_{C1}(t) - v_{C2}(t) - i(t)R_0$$

$$\frac{di_{Rn}}{dt} = -\frac{1}{R_n C_n} i_{Rn}(t) + \frac{1}{R_n C_n}$$

The SOC was then modelled within Simulink using Equation 22, while the power delivered over time is calculated using Equation 14. The MATLAB solver was set to variable step. The relevant results are retrieved from the simulations by writing a MATLAB script that retrieves the relevant data. Most of the data was stored as timeseries, while the current and voltage were retrieved as both arrays and timeseries. To describe the different characteristics of the battery, five different plots were made. These were SOC, power, current, voltage and voltage over current.

The other model was made to simulate the batteries over multiple cycles using a constant-current constant-voltage CC-CV system. The CC-CV system is a Simulink block that can be found in the simscape battery systems package. This block functions by enabling and disabling charging once a specific parameter is reached, while also defining the charging current, discharging current as well as the battery voltage. As the CC-CV block controls both charging and discharging, no resistive load was connected to the model.

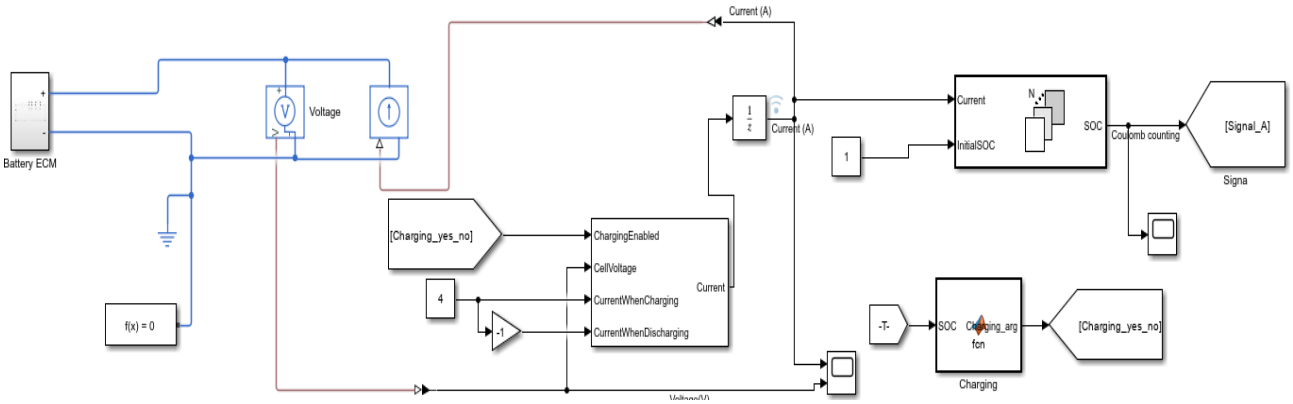


*Figure 12: Simulink for longrange operations*

The SOC was determined when the battery was charging and when it was discharging. The SOC in this model was calculated using a block that returned the SOC as shown in Equation 22. If the SOC was 0, the battery would start charging, and if the SOC was 1, the battery would start discharging. A simple for-loop was written to control this process. The maximum charge and discharge currents were set as the charging and discharging currents for the different batteries.

To be able to run the simulations accurately, the RC-parameters have to be determined and calculated. As there have been several studies into both NiMH and Li-ion RC parameters in the literature, it was decided to use the results from the literature as a basis when deciding the RC-parameters for the batteries presented in Table 2. The RC parameters to be decided was $R_0, R_1, R_2, C_1$ and $C_2$, while $\tau_1$ and $\tau_2$ were already known to be 10 seconds and 100-200 seconds [35]. It was decided to perform two different simulations for the discharge cycles with different $\tau_2$ values to see how much they affected the results. The relationship between the time constant and the RC parameters is given in Equation 27.

$$\tau_n = C_n R_n$$

*Equation 27: Time constant [38]*

$\tau_n$ is the time constant, $C_n$, is the capacitance for branch n, $R_n$ *is the resistance in branch n.*

The remaining of the RC parameters were determined by assuming the batteries chosen had the same RC-parameters that have previously been found in the literature. For the lithium battery the RC-parameters are given in Table 3. For the NiHM battery the RC parameters are given in Table 4. As $\tau_1$ was set to 10 seconds in the literature while $\tau_2$ varied, it was decided to

test how the different $\tau_2$ affected the battery models. Case 1 refers to when $\tau_2$ = 100 seconds and case 2 refers to when $\tau_2$ = 200 seconds.

*Table 3: RC- Parameters with different time constants for lithium batteries*

| Li-Ion battery | $\tau_2$ = 100 seconds | $\tau_2$ = 200 seconds | Source |
|---|---|---|---|
| R0 | 0.03 | 0.03 | [43] |
| R1 | 0.02 | 0.02 | [43] |
| R2 | 0.03 | 0.03 | [43] |
| $\tau_1$ | 10 | 10 | [35] |
| $V_{ocv}$ | 3.7 | 3.7 | datasheet [44] |
| C1 | 500 | 500 | Equation 27 |
| C2 | 5000 | 6666 | Equation 27 |

The same was done for the NiMH and is summarized in Table 4

*Table 4: RC-Parameters with different time constants for NiMH batteries*

| NiMH battery | $\tau_2$= 100 seconds | $\tau_2$ = 200 seconds | Source |
|---|---|---|---|
| R0 | 0.11 | 0.11 | [45] |
| R1 | 0.01 | 0.01 | [45] |
| R2 | 0.01 | 0.01 | [45] |
| $\tau_1$ | 10 | 10 | [35] |
| $V_{ocv}$ | 2.4V | 2.4V | datasheet [46] |
| C1 | 1kF | 1kF | Equation 27 |
| C2 | 10kF | 15kF | Equation 27 |

After applying the simulation parameters into the models, the simulations were then performed. The signal being sent to both batteries started as a high load, which gradually declined over 1000 seconds. This is shown in Figure 13.

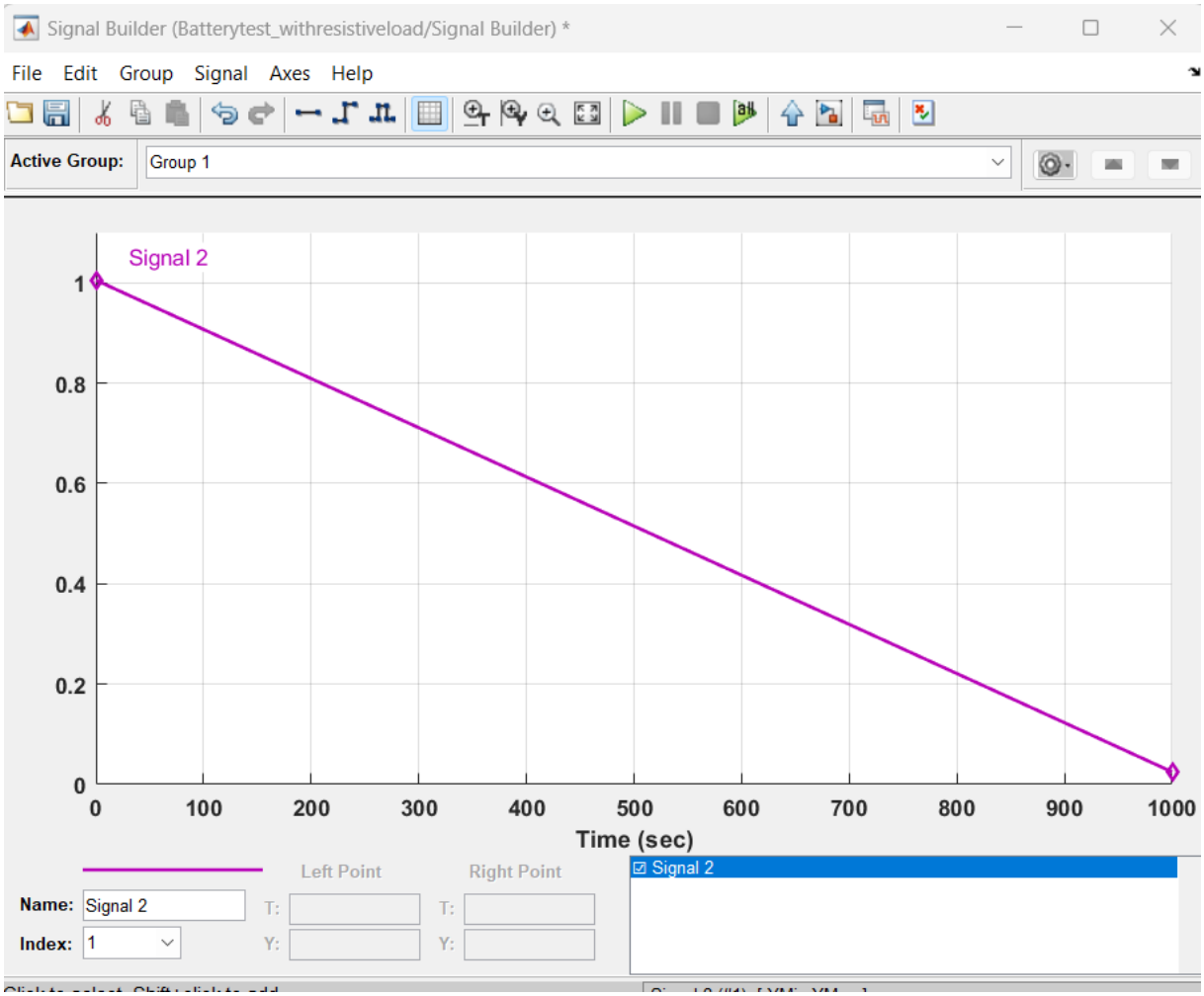


*Figure 13: Resistance signal in Simulink*

For the long range simulations a CC-CV method was applied where the SOC controlled the cycles. For the Lithium battery where the maximum charging current and discharging current were given, those values were used. For the NiMH battery only the maximum charging current was stated, so it was assumed that the maximum current was the same for charging and discharging. In Table 5 the relevant currents for the batteries are given.

*Table 5: Relevant input for simulation*

| Battery | Li-ion | NiMH |
|---|---|---|
| $I_{charge}$ | 2.6 A | 1 A |
| $I_{discharge}$ | 5.2 A | 1 A |
| Capacity | 2.6 Ah | 2.0 Ah |

## 3.3 Deriving a model for supercapacitors

There are many different types of models for supercapacitors that have been presented in the literature. Equivalent circuits are some of the most common models for supercapacitors. L. E Helseth [47] studied some of the limitations of using RC-circuits when modelling supercapacitors. These branches lack some of the required properties to explain the long-term behaviour of the supercapacitor [47]. In order to have the most accurate models for supercapacitors, a dynamical equivalent circuit model should be utilized according to L. E Helseth [47]. However, these models are more complex and requires further data from the frequency and time domain [47].

Khaled et al. [48] performed a literature review of different models for supercapacitors. The different models being used for modelling supercapacitors could be divided into electrochemical models, equivalent circuit, intelligent models, fractional models, self-discharge models and thermal models [48]. All these models range in varying complexity while also capturing different parts of the electrochemical properties that supercapacitors have [48]. These models are often used in management systems for supercapacitors. Which application the supercapacitor is being used for, will define which model complexity is required.

R. Faranda [49] presented a simplified version of an equivalent circuit that was easier to parameterize compared to other models discussed in the literature. The model discussed by Faranda is a two branched model which also has a methodology that has been derived when the RC parameters shall be found. The model in [49] focuses more on the electrical behaviour of the supercapacitor. For long term simulations these models are not necessarily the most accurate. This is due to simplifications being performed to the model. The method proposed by R. Faranda was easy to build in Simulink, while different RC-parameters were also suggested in the paper. The model proposed assumes that there are some non-linear parts, but these will be assumed to be linear in the model used in this thesis.

The RC-parameters for supercapacitors take into consideration factors like electrode resistance, electrolyte resistance, pore size, membrane porosity and the resistance due to connecting electrode-collectors [49]. The equivalent circuit model that R. Faranda proposed is

shown in Figure 14. Ci1 in the model proposed by R. Faranda is often modelled as a non-linear capacitor, but in this thesis a linear capacitor was used to simplify the circuit.

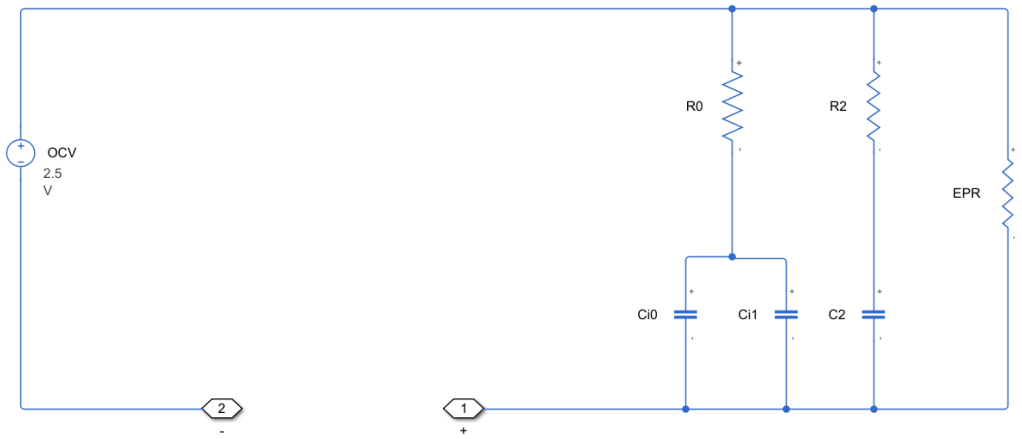


*Figure 14: Equivalent circuit model for supercapacitors. Adapted from "A new parameters identification procedure for simplified double layer capacitor two-branch model", R. Faranda, Electric power systems research, volume 80, 2010, p 363-371. Reprinted with permission. Copyright Elsevier [49]*

Two different supercapacitors were found on the internet to be modelled further. These were a Nichion 150F supercapacitor and an Eaton 400F supercapacitor. Some of the properties for both are shown in Table 6. These were chosen as the datasheets from the manufacturer had all of the required parameters readily available. Both brands are also well known.

*Table 6: Supercapacitor properties*

| | Nichion 150F | Eaton 400F | Source |
|---|---|---|---|
| V_max | 2.5 V [50] | 2.7 V [50] | Datasheet |
| Capacitance | 150F [50] | 400F [50] | Datasheet |
| Equivalent series resistance | 22 mOhm [50] | 3.2 mOhm [50] | Datasheet |
| Maximum energy | 468J | 1458J | Equation 17 |
| Current charging | 1 A | 4 A | Assumed |
| Capacity | 0.10 Ah | 0.3 Ah | Equation 18 |

The next step was then to determine the RC-parameters for the supercapacitors. It was assumed that R0 was the same as the series resistance that was provided in the datasheets. If the supercapacitors are discharged in a lab, then R0 can be calculated by dividing the change of voltage over the charging current [49]. The time constant for supercapacitor modelling is often set to about 240 seconds [49].

The remaining parameters that have to be determined are then Ci1,C2,R2 and the equivalent parallel resistance (EPR). The EPR can be calculated using Equation 28.

$$EPR = \frac{V_n}{I_{leak}}$$

*Equation 28: Equivalent parallel resistance [49] [38]*

EPR is the equivalent parallel resistance, $V_n$ is the nominal voltage and $I_{leak}$ is the leakage current

Some assumptions were made for the rest of the parameters for the supercapacitors. Assuming the capacitor is behaving non-linear, the rest of the RC-parameters can be calculated using Equation 29.

$$C_0 = c_1 I_c$$

$$k_v = 2c_2 I_c$$

*Equation 29: RC-parameters for first RC-branch [49]*

To calculate the constants c1 and c2, R. Faranda established a system of equations that needed to be solved. Some of the input required for the system of equations are determined by reading of two different points along the charging curve for the supercapacitor. The voltage and the time should be noted for both the points. It's important to try and scatter the points so that most of the charging curve is covered in between those points [49]. R. Faranda then showed that C0 can be calculated using Equation 30.

$$C_0 = (\frac{t_1}{V_1} - \frac{V_1 t_2 - t_1 V_2}{V_2^2 - V_1 V_2})I_c$$

$$k_v = 2(\frac{V_1 t_2 - t_1 V_2}{V_1 V_2^2 - V_2 V_1^2})I_c$$

*Equation 30: C0 and kv for a supercapacitor RC branch [49]*

t1 is the time at point 1, $V_1$ is the voltage in point 1, $t_2$ is the time in point 2 and $V_2$ is the voltage in point 2.

As it was assumed that the second capacitor in the RC-branch was linear, the equation for $k_v$ cannot be used directly as input in Simulink. It was assumed that the capacitance for the supercapacitor in the kv branch was constant and less than $C_0$. This was done as no charging curves for the different supercapacitors were found, and no experiments were performed in this thesis. R. Faranda conducted several experiments for a number of supercapacitors which show the order of magnitude that can be expected for the RC parameters. The literature gives some indications as to the magnitude of the parameters. By using Equation 27 the resistance in the second branch can be found. The parameters for the different supercapacitors were then estimated based on what could be found in R. Faranda [49]. This is summarized in Table 7. Even though Equation 29 and Equation 30 were not directly solved when assuming the parameters, they were presented as they show what properties affect the RC parameters for the supercapacitors.

*Table 7: RC-Parameters for Supercapacitors*

| Parameter | Nichion S.C 150F | Eaton 400F S.C | Source |
|---|---|---|---|
| V_max | 2.5V [50] | 2.7 V [51] | Datasheet |
| $\tau_2$ | 240s | 240s | R. Faranda [49] |
| R2 | 10 ohms | 3 ohms | Equation 27 |
| $C_1$ | 35 F | 132 F | Assumed |
| $C_2$ | 24 F | 80 F | Assumed |
| $C_0$ | 150 F [50] | 400 F [51] | Datasheet |
| EPR | 5000 | 5000 | Equation 28+R Faranda [49] |
| R0 | 0.022 [50] | 0.03 [51] | Datasheet |
| $I_c$ | 1 A [50] | 1 A [51] | Datasheet |

For the discharge cycle of the supercapacitor the same resistive load as for the batteries was utilized. The full model in Simulink is shown in Figure 15. The simulation stops after the SOC reaches 0 based on Equation 23. The power, current, voltage, the SOC and the current over voltage are then plotted by using timeseries and arrays as output.

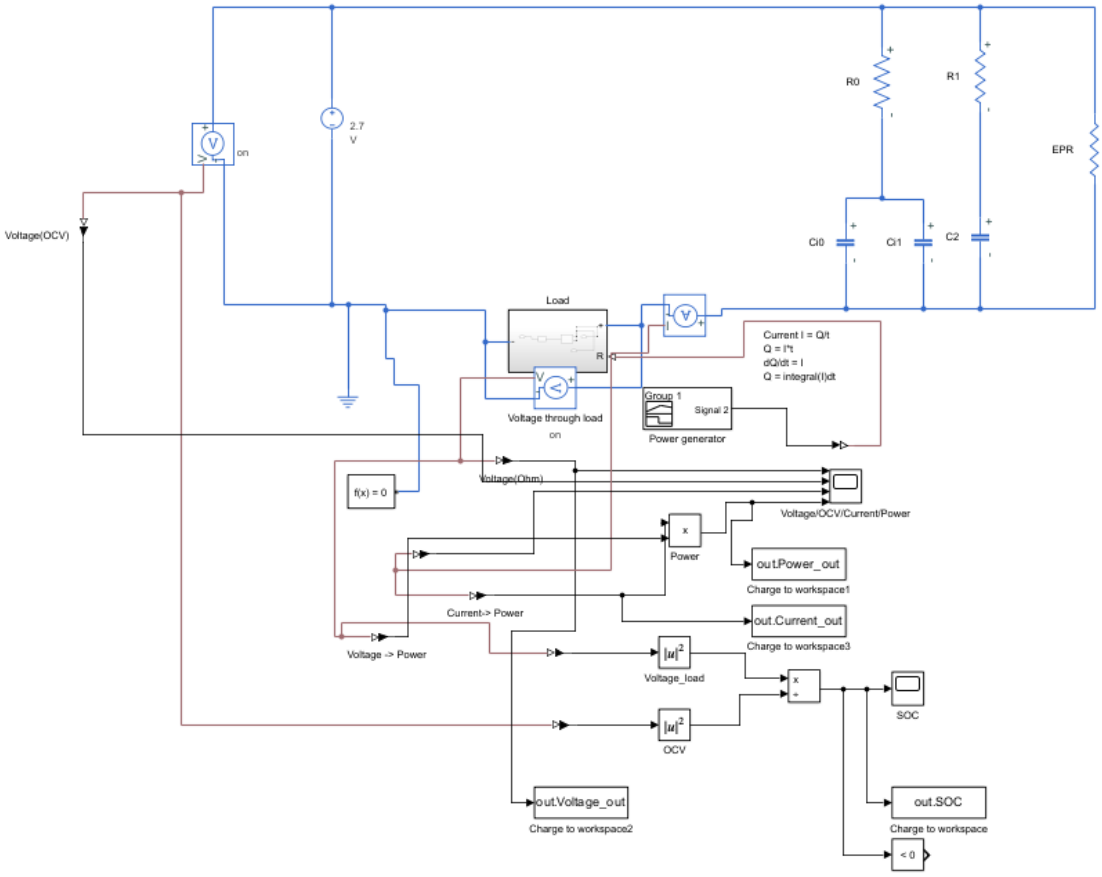


*Figure 15: Supercapacitor full model in Simulink*

The long-range model is based on using the battery CC-CV charging block in Simulink, as was chosen for the batteries. Due to receiving negative voltage numbers during the long-range simulation, it was decided to normalize the voltage during charging. Coulomb counting method was chosen for the supercapacitor long-range simulation as well since its implementation was easier.

## 3.4 Comparison parameters and weight

### 3.4.1 General

Due to the models requiring different input parameters, it is important to determine how much this affects the model output. The discharge models were tested, and it was noted how the cycle lifetime was affected by the different parameters.

### 3.4.2 Battery

For the parameter testing of the batteries the voltage was set to 3.7 V. The parameters are summarized in Table 8. It was decided to see how changing these parameters affected the SOC and the cycle time during discharging. Using these parameters, the cycle time was 895 seconds. The SOC was gradually decreasing linearly as the simulation ran.

*Table 8: Battery parameters for testing*

| Parameter | Value |
|---|---|
| R0 | 0.04 |
| R1 | 0.02 |
| R2 | 0.03 |
| C1 | 500 |
| C2 | 6666 |

To see how the different parameters affected the battery model, R0,R1 and R2 were all increased. C1, C2 and C0 were all decreased. This is summarized in Table 9.

*Table 9: Battery parameters testing*

| Parameter | Value | Estimated cycle time |
|---|---|---|
| R0 | 0.09 | 733 s |
| R1 | 0.1 | 740 s |
| R2 | 0.1 | 706 s |
| C0 | 250 | 692 s |
| C1 | 2500 | 694 s |

It was observed that increasing the resistances decreased the cycle time of the battery gradually. The most severe effect to the battery cycle time was decreasing the capacitances in the RC branches in the model. In Figure 16 the SOC is plotted when C1 was changed. It was seen that the cycle time in the battery model was more affected by changes of parameters than the shape of the SOC curve.

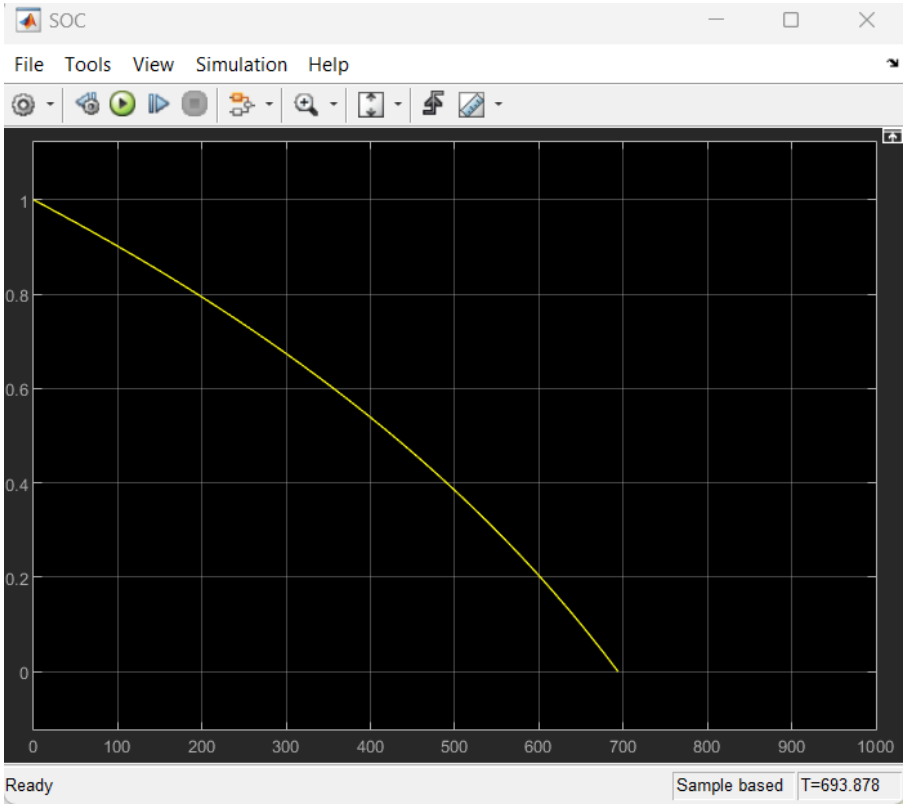


*Figure 16: SOC over time when C1 = 2500*

### 3.4.3 Supercapacitors

For the parameter testing of the supercapacitors the voltage was set to 2.7 V. The rest of the parameters are summarized in Table 10. If R0 is changed, it was assumed that the rest of the parameters are kept identical as in Table 10. The cycle time using the parameters in the table below was about 400 seconds.

*Table 10: Constant parameters during estimation*

| Parameter | Value |
|---|---|
| R0 | 0.03 ohm |
| EPR | 5000 ohms |
| C0 | 89 |
| C1 | 29 |
| R1 | 1 |
| C2 | 13.71 |

In Table 11 below it was tested how increasing R0, EPR affected the cycle time.C0, C1 and C2 were all decreased to see how they affected the simulations.

*Table 11: Parameter test values*

| Parameter | Value | Estimated cycle time | Notes |
|---|---|---|---|
| R0 | 0.3 | 350 s | Increased activation losses |
| EPR | 7500 | 300 s | More linear SOC fade |
| R1 | 3 | 300 s | Curvy SOC fade |
| C0 | 60 | 250 s | Curvy SOC fade |
| C1 | 16 | 250 s | Curvy SOC fade |
| C2 | 2 | 250 s | Curvy SOC fade |

It was observed that if the ESR was increased to 7500 ohms, while keeping all other values constant, the decay of SOC would be more linear when compared to the other SOC profiles. Such profiles indicate thar ir losses are more dominant. When R0 was increased, it was witnessed that the activation losses were more dominant at the start of the process. This can be observed by the rapid drop of voltage during the initialization of discharging. The cycle time was estimated to be the parts of the SOC curve where the supercapacitor delivers useful energy. In Figure 17 the SOC curve when the ESR is 7500 is shown. Figure 18 shows the SOC curve when R0 = 0.3.

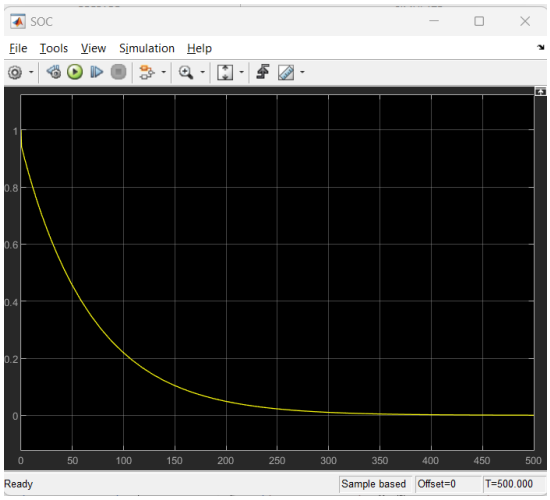


*Figure 17: SOC(t) for different parameters when ESR = 7500*

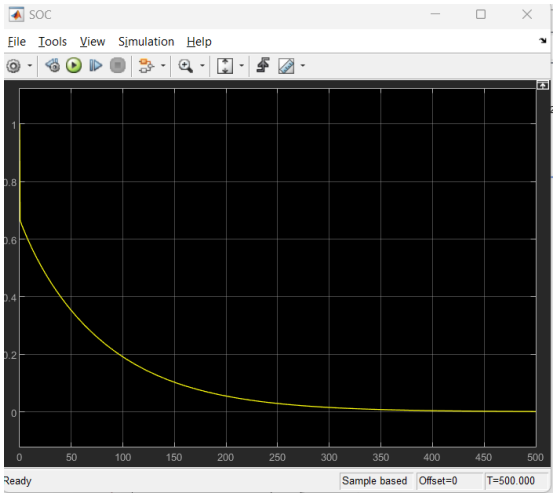


*Figure 18: SOC(t) when R0 = 0.3*

## 3.5 State of health estimation

To obtain the SOH over time some assumptions had to be made. Firstly, it was assumed that the degradation occurred linearly, and that the battery and the supercapacitor were fully charged and discharged for every cycle. Secondly, it was assumed that the temperature was constant at 25 degrees and that there was no temperature and heat transfer in the charging/discharging process. Lastly, any effect of gassing and slow diffusion on aging was neglected. It was assumed that once the battery/supercapacitor reached a SOH of 80%, it would be at its end of life (EOL) point. It was assumed that the aging parameter considers all the aging processes. There are two main processes that occurs in batteries and supercapacitors when they age. These are capacity fading and increasing internal resistance [52]. To model the SOH over time, it was assumed that the resistance in the energy storage device was the main cause of health degradation. It was assumed that this effect increased linearly. The maximum power was obtained from the simulations during CC-CV operations. By using Equation 24, the SOH was then modified and modelled using Equation 31.

$$SOH = \frac{P_{actual}(n) - I^2R}{P_{max}}$$

*Equation 31: SOH model applied*

$P_{actual}(n)$ is the actual power at cycle n, $I^2R$ is the power loss due to degradation. $P_{max}$ is the max power

# 4 Results and discussion

## 4.1 Limitations

The models presented in this thesis has their limitations. Before discussing the results, it is important to analyse some of these limitations for both the battery and supercapacitor models. For both models the following assumptions were made:

- No heat transfer was present
- There was a constant temperature of 25°C
- Battery and supercapacitor degradation was linear
- RC-parameters were estimated based on the order of magnitude seen in the literature
- There was no pseudo capacitance
- The relationship between capacitance, current, voltage and current followed a linear relationship with continuous derivatives
- Linear degradation

Batteries and supercapacitors have a variety of physical phenomena that occurs during the operating phase. Due to the limited number of RC-pairs used, not all of the physical phenomena can be accurately captured and modelled. Also, RC-parameters found in the literature might not accurately reflect the exact batteries/supercapacitors found online.

## 4.2 Bugs and issues encountered in MATLAB

During the simulations there were discovered some bugs and issues in the models that were not due to the assumptions made. Some of these bugs and issues were:

- The for-loop written to control charging and discharging would often return the wrong value after one cycle. This was mitigated by adding further conditions to the SOC for-loop
- The coulomb counting block gave negative SOC. This was mitigated by normalizing the SOC calculations before going into the for-loop
- The voltage of the supercapacitor would often give negative values. This was adjusted by normalizing the voltage
- The MATLAB solver broke down after about 10000 seconds for the supercapacitors and 3600*10 seconds for the batteries. Therefore, the long-range simulations for supercapacitors were 10000seconds and batteries were 3600*10 seconds

## 4.3 Literature review

### 4.3.1 Discussion of literature findings

The findings in the literature suggest that both batteries and supercapacitor have different strengths and weaknesses. Both batteries and supercapacitor are being used in the same areas for energy storage. The most dominant issue that was seen for batteries was that the charging time was quite long. The increased cost of electricity might come from not having the battery ready for when the system required the maximum output. Some of the other downsides of batteries were shown to be that the weight and size of the system were quite large. For some applications weight is not a good trait as it might remove some flexibility of other aspects of a system. An example of this might be electric vehicles. Here increasing the weight of the battery system might increase the range of the car to some point, but eventually lead to the range of the car decreasing again.

For supercapacitors the main issue seems to be the amount of energy that can be stored at the time. For grid purposes the high power bursts a supercapacitor can give might be good for sudden changes in demand, but for a system where constant power is required, a supercapacitor might not be the optimal choice for that application. Supercapacitors used in buses as done in Shanghai in 2010 might have some disadvantages. As these buses were only used in the World Expo, the area they needed to travel was limited. The flow of traffic was known and could be controlled. For a bus driving in a place where the traffic varies, with large ques and where accidents can happen, the bus might need to have a larger charge or a reserve system. If one bus is delayed and have to charge the supercapacitor bus might be causing a que at the charger for other buses, making the delay even longer.

In order to mitigate some of the disadvantages that the literature addresses for both systems, hybrid energy systems can be used. As batteries are able to provide a stable discharge cycle while supercapacitors have a more pulse like discharge shape, supercapacitors are more useful for short burst and batteries for constant loads. By combining batteries and supercapacitors the system will therefore be able to handle both short bursts and long constant loads. This combination provides a storage system that is better equipped to handle most of the load situations that might occur in different applications.

## 4.4Simulation of lithium batteries

### 4.4.1 Case 1

The differences between case 1 and case 2 were marginal. Therefore, the results of case 2 of the lithium batteries were placed in Appendix A: Li-ion simulation Case 2. The relevant discussions therefore apply to both cases.

In Figure 19 the SOC(t) for the lithium-ion battery during case 1 is shown. This was produced with a resistive load instantly starting on a high value, and then gradually decreasing the load over 1000seconds. In Pai et al. [53] a similar curve for SOC was seen. The load in Pai et al. [53] was varying, but overall, the load followed a similar trend line as was used in this thesis. The battery simulated in Pai et al. [53] however lasted longer. This might be due to them having a battery with a higher capacity than simulated in this thesis. By having more cells in series or parallel, the cycle life can be increased.

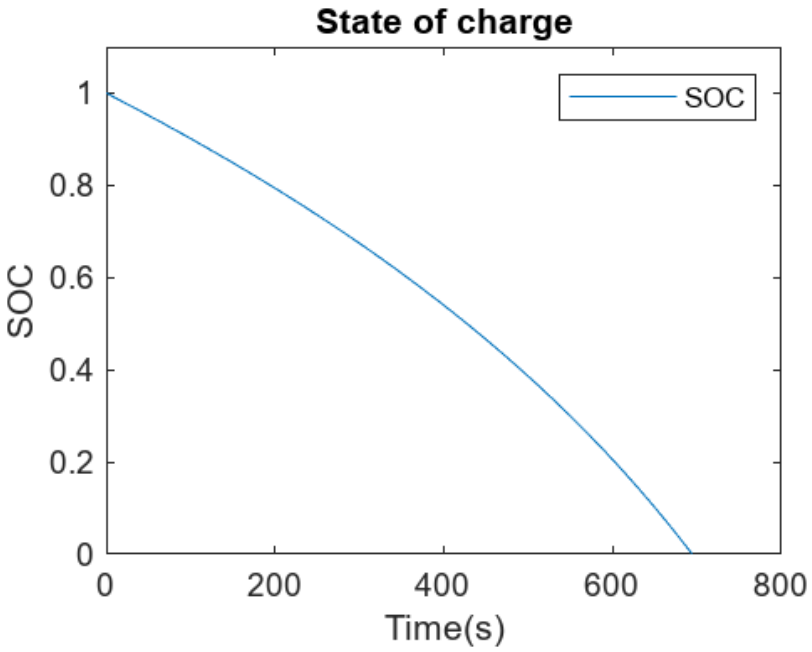


*Figure 19: SOC for the lithium battery*

The power for the battery was plotted in Figure 20Figure 19, while the current was plotted in Figure 21. Due to the relationship shown in Equation 14, the power can be seen as proportional to the current. The huge spike of current and power at the end of the cycle might

be due to an electrical overload. As the resistive load starts high and gradually is reduced, it allows for more current to flow through the circuit. By using a resistive load with a resistance profile as shown in Figure 13, the Li-ion battery was able to provide a charge for about 12 minutes before reaching a SOC of 0 and then stopping. Based on the information in the data sheet the maximum discharge current of the battery is 5.2 A. The equivalent circuit models gave a maximum current of 8.4 A. This will damage the battery. The battery can be damaged by the over-current increasing temperatures, causing side reactions and gassing [7]. This might also indicate that the slope of the resistive load was set too steep for the system to handle without an external BMS system. The jump in the beginning of the cycle is caused by the battery instantly responding to a load higher than 0. This causes the current to not gradually increase, but to start higher than it would have if the resistance increased gradually from 0.

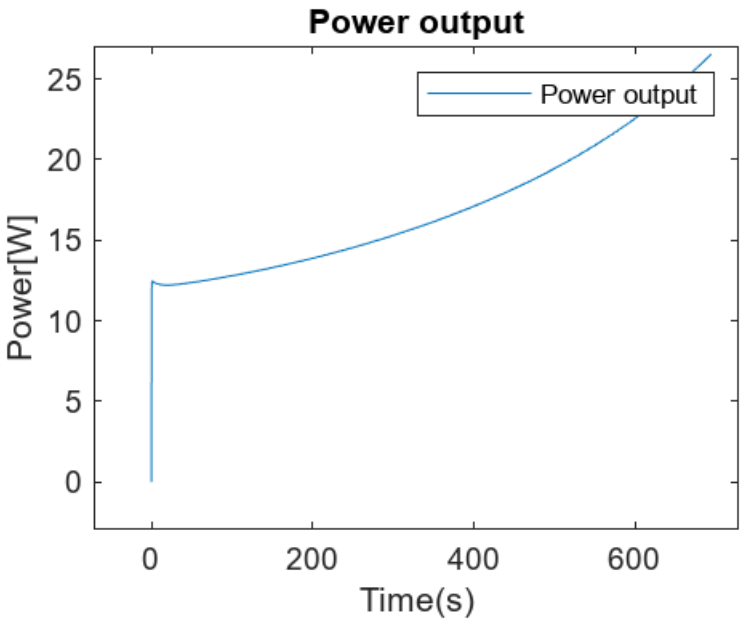


*Figure 20: Power output for the lithium battery*

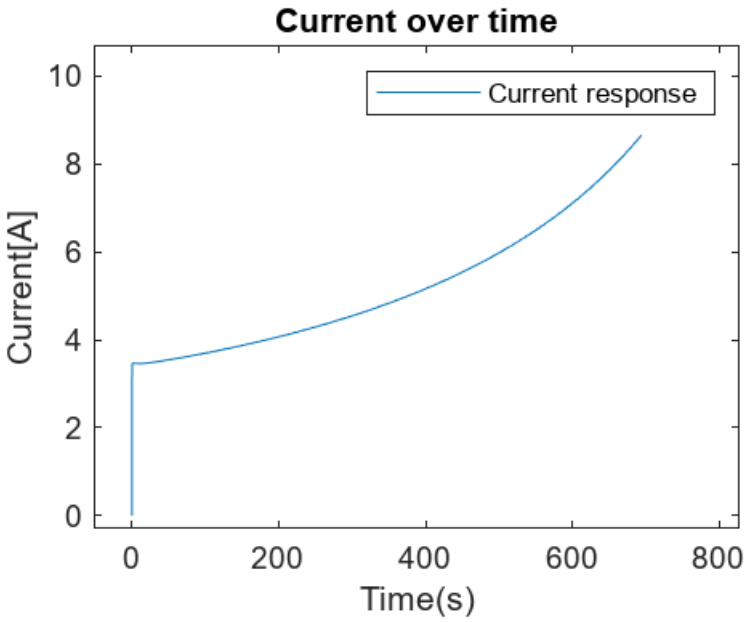


*Figure 21: Current response for the lithium battery*

The voltage over time was then plotted and is shown in Figure 22. The shape is as expected. A similar curve was seen in Casanova et al. [54]. However, the model proposed in Casanova et al. [54] was with a single resistor. The model used here captures better the activation and ohmic polarization compared to Casanova et al. [54] The activation polarization can be seen as the first initial rapid drop of voltage right at the beginning of the discharge. The ohmic losses are the linear part seen between about 3.5-3.2 V as seen on the y-axis. The concentration polarization was expected to make a more rapid drop than the plot shows. In Dell [7] and Casanova et al. [54] the concentration losses are modelled as a more abrupt drop of voltage. This was also highlighted in Figure 3 where the voltage drops more rapidly. This can also imply that this battery is not as affected by concentration polarization during a gradual decreasing load as other batteries.

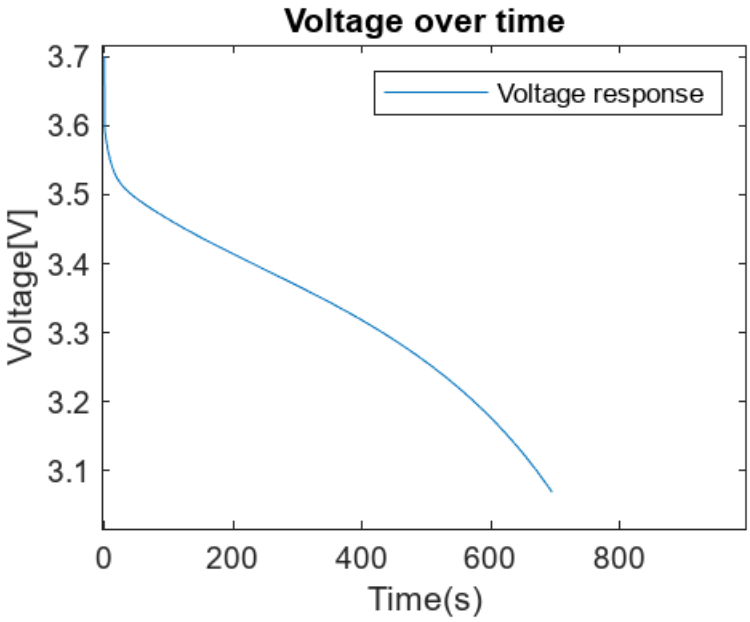


*Figure 22: Voltage over time for the battery*

There are different aspects of the model that may cause this. As the models are assuming a constant temperature, the effect an increasing temperature has on the reactions within the battery, is neglected. As the temperature is increasing during the reaction, it is expected that $\Delta G$ will be reduced as seen in Equation 5. This reduces the amount of work and potential the battery can give. The reduced potential is also seen in the Nernst equation. The second part of the Nernst equation is $-\frac{RT}{nF} ln\ (K)$ and highlights that the potential the battery can give will be reduced as the temperature T is increased over time. The temperature also influences the equilibrium constant [10] [8] [9]. As electrochemical reactions in batteries are exothermic, the magnitude of K will decrease once the temperature of the battery starts to increase [10] [11]. This might change the slope and dynamics within the battery.

A second characteristic seen in the plot is that the battery does not reach the cut-off voltage advertised by the datasheet. This might be due to the RC-parameters being estimated by assuming the RC-parameters are like a battery of a similar chemistry that was derived from the literature. The difference might also occur due to the cut-off voltage that the battery was rated for was 2.75 V at 0.2 C (5-hour). Using Equation 11 this gives a current of 0.52 A. Based on the current over time plot the current achieved during the discharge test was substantially higher than the current the cut-off voltage was rated for. By having a varying current, the cut-off voltage for this battery at 3C is then roughly 3.1 V. This is a very high C-rate that will damage the battery based on the information from the datasheet. High current might be used for

acceleration of electric vehicles, or frequency regulation of the grid [14]. As seen on the current and voltage plot, the area where the most current is given is when the concentration polarization is the main loss factor. If this battery is used for this purpose the main issues that must be dealt with will then be the concentration polarization [7]. The curve for the concentration losses might also not be visible due to using a capacity that is off compared to the actual capacity of the battery with the RC-parameters used. This might cause the SOC to reach 0 before the true SOC of 0 would have been reached. This might cause the simulation to stop earlier than it would have, and not revealing the true magnitude of the concentration losses.

The voltage as a function of current was then plotted in Figure 23. In Jung. Ki Park [12] a similar linear plot was seen for a lithium battery with an increased current density. The current plot shown here shows for the first Amperes that the main polarization might be ohmic. At about 4 Amperes the concentration losses become more relevant and is the main polarization. For a battery it is expected that the voltage will have a more sudden drop in the beginning due to concentration issues. This drop was also seen in Jung Ki Park [12]. It is expected that the voltage loss during increased current will take the same shape as Figure 20. As the equivalent circuit models are not batteries, but a series of electrical components that try to represent some of the dynamics of the battery, some physical phenomena will not necessarily be captured. The shape of the plot might indicate that ohmic losses and concentration losses are more dominant for loads which start high and is gradually decreasing.

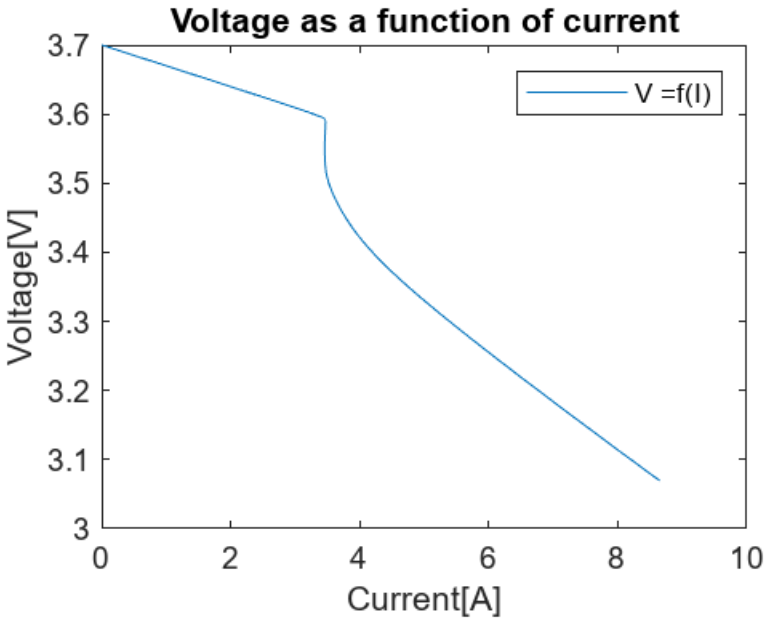


*Figure 23: Voltage as a function of current*

### 4.4.2 Long range

The long range results were then plotted by using a CC-CV block. In Figure 24 the power over time is plotted. Figure 25 and Figure 26 show the current and voltage response over time. Based on the datasheet the charging current was set to 2.6 A and the discharging current was set to 5.2 A. Based on the plots the charging time for the battery at 2.6 A is almost an hour. As the current for charging is lower than for discharging, the power required to charge is less than the power the battery provides during discharging. The minimum and maximum voltage seen in the simulations do not match with the maximum and minimum voltage provided in the datasheet. During charging the voltage goes above the OCV. This is expected due to the polarization as discussed in Equation 15. During charging the sign of all the polarization changes which then leads to the system requiring more voltage during charging then what the battery can deliver. During the simulation time of 3600*10seconds the battery performed 8 full cycles.

In this simulation the battery started fully charged and was then discharged. Once the battery reached about 3.25 V, the SOC reached 0 and a low current was first applied. This low current helps reducing some of the resistance [7]. After some time, the battery charger applied its maximum current, and charged on a constant current until it reached 3.9 V. The constant

current can be seen as the straight line in Figure 25. The battery was then charged with a constant voltage until it reached its OCV which is the rapid drop in current that can be seen in the same figure.

A similar shape was seen in Rad et al. [55]. The model proposed in Rad et al. [55], however, also investigated the temperature dependence of the lithium battery during charging and discharging. As previously mentioned, this was not done in this thesis. The main differences between the plots in Rad et al. [55] and the plot in this thesis is that the voltage drop during discharging in Rad et al. [55] was spikier at the end points. The voltage drops seen in Figure 26, however, do not have a spike, but are constant at 3.25 V. This might be due to different assumptions regarding temperature. The temperature set in Rad et al. [55] was T = 40°C and with heat transfer included in the model, while this model assumed a constant temperature of T = 25°C. This might affect the dynamics of the battery as previously mentioned and might be the reason that the spike in Rad et al. [55] is not present in this model during CC-CV operations. A spike was seen in the power plot in Figure 24.

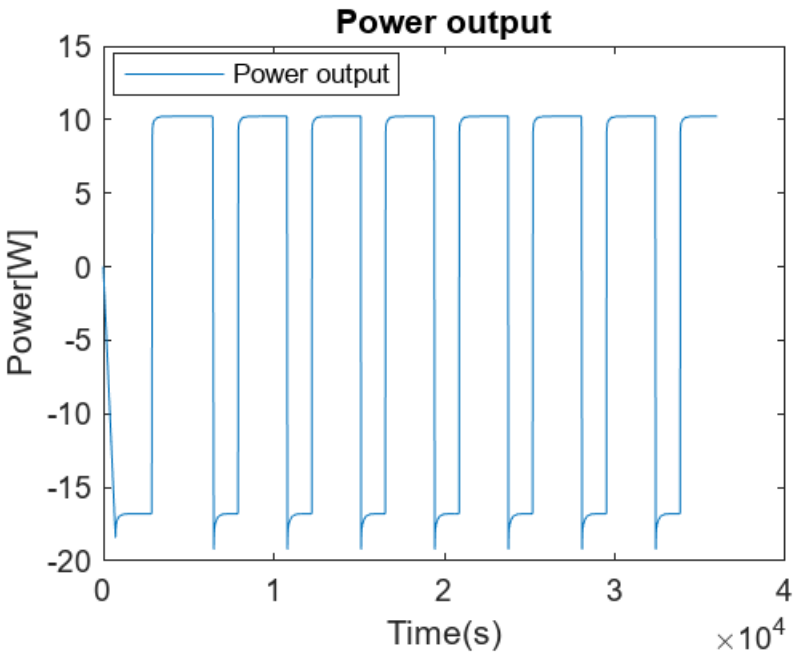


*Figure 24: Power output during long range operations (Li-ion battery)*

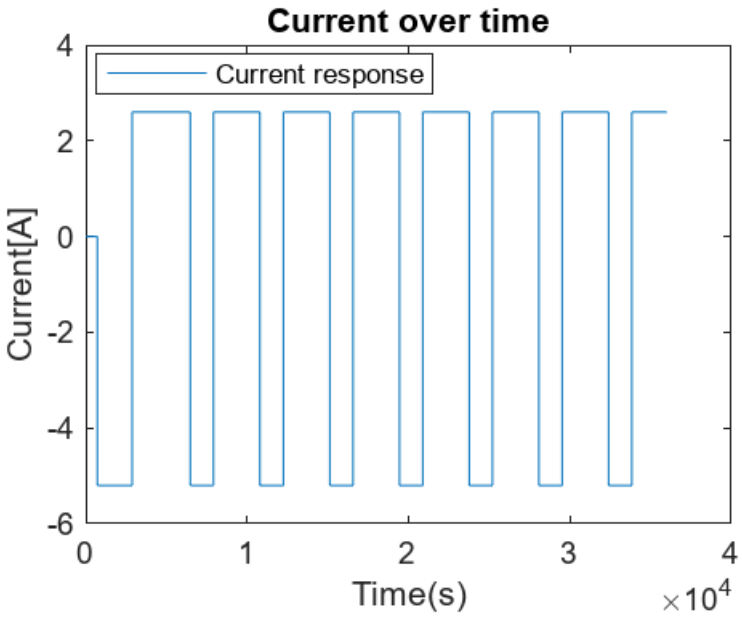


*Figure 25: Current over time during long range operations (Li-ion)*

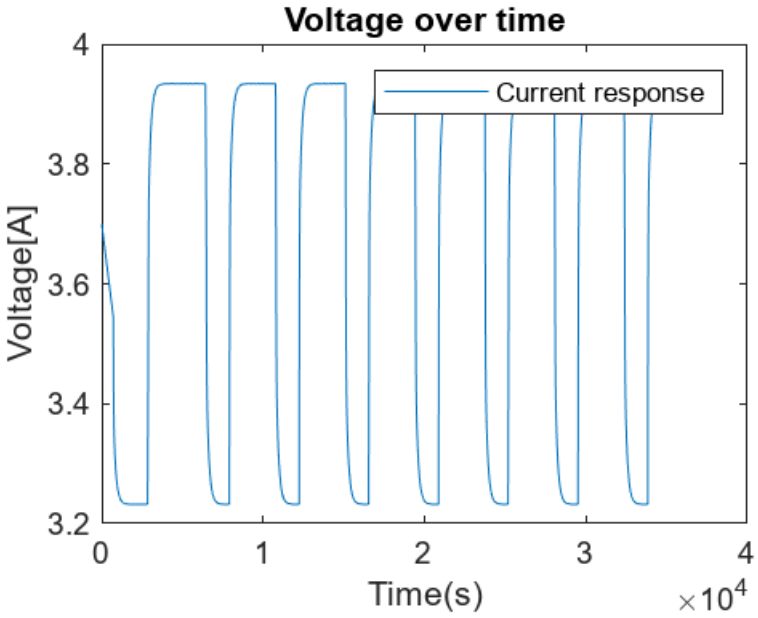


*Figure 26: Voltage over time during long range operations(Li-ion)*

## 4.5 Simulation of NiMH batteries

### 4.5.1 Case 1

All the plots for case 1 and case 2 for the NiMH battery were similar. Case 1 was therefore chosen to be discussed. The points brought up in this section still apply for the plots in case 2. The plots for case 2 for the NiMH batteries can be found in Appendix B: NiMH battery simulation case 2.

The SOC for the NiMH is plotted in Figure 27. The plot shows that the SOC is gradually declining over time as the load is decreased. The cycle time during the discharge test for the NiMH battery was about 850 seconds before the battery was depleted. The plot follows the same structure as the Li-ion battery, but had a longer cycle life.

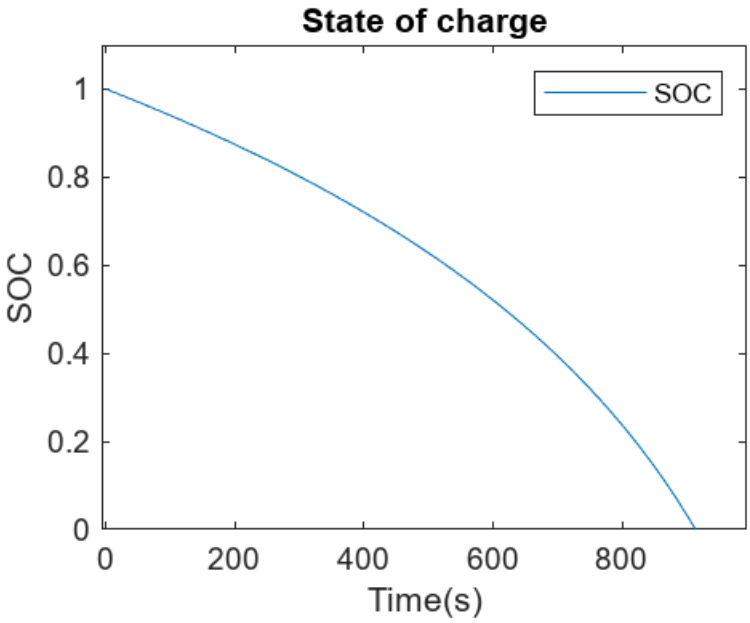


*Figure 27: SOC over time for the NiMH battery (case 1)*

The power and current were then plotted in Figure 28 and Figure 29. Compared to the lithium battery the NiMH battery had the same current response as the lithium battery, but had a lower power output. This is due to the voltage being generally lower than for the lithium battery.

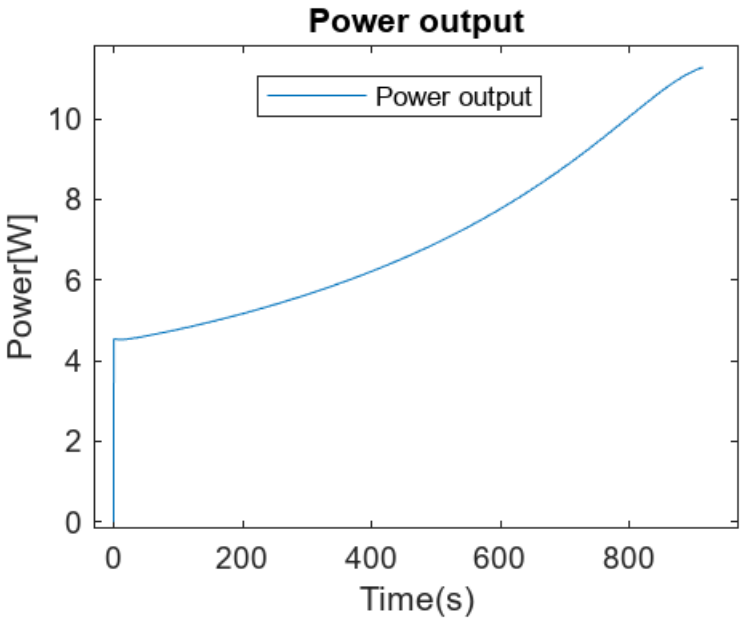


*Figure 28: Power output NiMH battery (case1)*

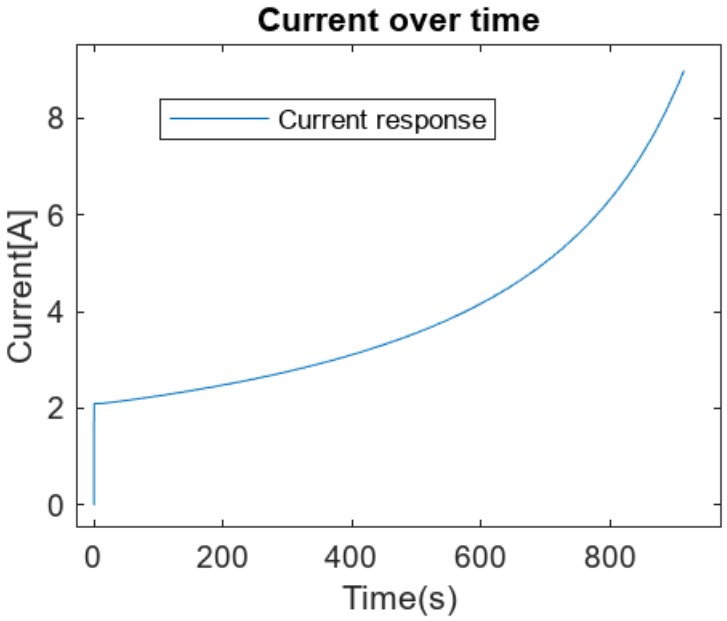


*Figure 29: Current over time NiMH (case 1)*

Figure 30 shows the voltage over time for the NiMH battery. In Dell [7] a similar plot is shown where the voltage the battery can give over time is stable until the battery comes to the point where the concentration issues cut the rest of the voltage. This was also seen in Krishnamoorthy et al. [56]. This tendency can also be seen in the plot from the model. The activation polarization is a little less than for the lithium battery, but it is still clearly visible. Based on the plot the ohmic losses are less than for the lithium battery, which can be seen for

a voltage between 2.19 V and 1.8 V. After the voltage has reached about 1.8 V, the concentration polarization becomes the dominant loss. It is worth noting that a NiMH often has a cut-off voltage of about 1.0 V [7]. In the datasheet for the battery simulated it is noted that the battery has multiple cells, giving a higher voltage than what a single NiMH-cell delivers. When compared to the lithium battery, the NiMH-battery is also less prone to damage caused by over discharging.

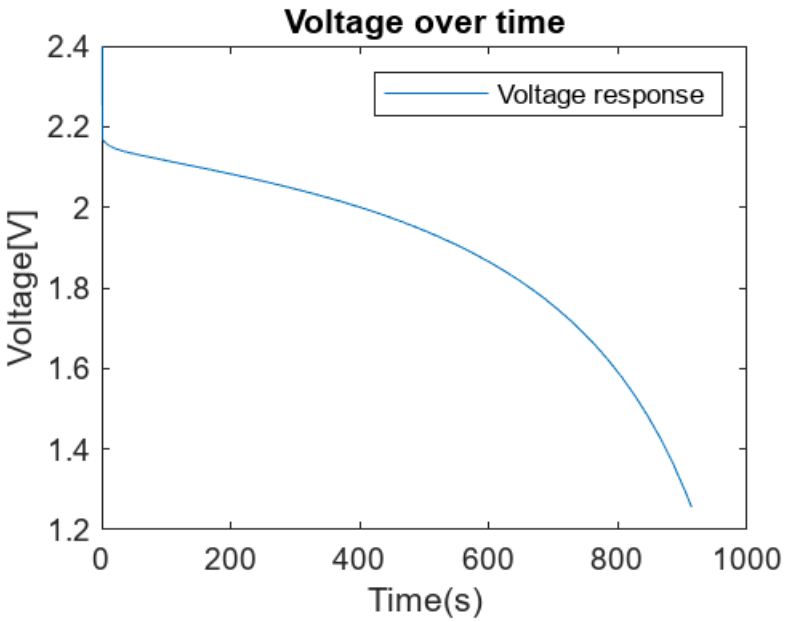


*Figure 30: Voltage over time for the NiMH battery (case1)*

NiMH batteries are also sensitive to heat. As the model assumes no heat transfer, the actual discharge curve with heat transfer included as well is needed to increase the accuracy of the model. As previously discussed in the section for lithium batteries, the same applies here regarding heat transfer and dynamics taking place within the battery.

The voltage over current seems to be linearly dependent on each other than for the lithium battery. This is seen in Figure 31. Based on the current in Figure 29 and the voltage in Figure 30 the voltage and current are inverse proportional to each other. This means that as the current is increased, the voltage is decreasing. Figure 31 then shows that this proportionality has a linear relationship. This is due to there not being any heat transfer models, and that the resistance is constant in the RC-parameters during the discharging cycle. The cause of this

might also be the choice of using linear dependant equations for the different components in the equivalent circuit model. Both Equation 20 and Equation 21 are linear differential equations. Equation 20 shows that the current through a capacitor is proportional to the derivative of  the voltage over time, while the voltage through an inductor is proportional to the derivative of the current with respect to time.

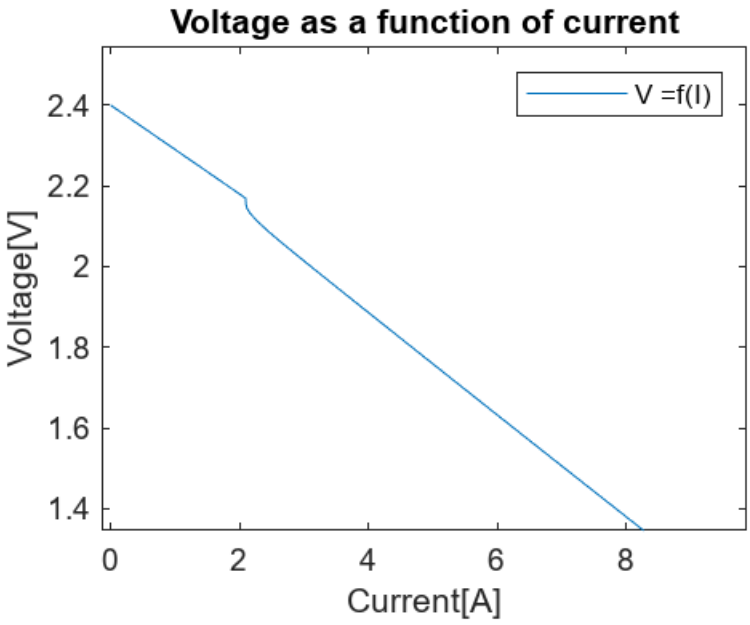


*Figure 31: Voltage as a function of current NiMH*

### 4.5.2 Long range

The long-range simulations for the NiMH batteries were then performed using the same block as the Li-ion battery. The NiMH battery was able to give 8.5 cycles over the time of 3600*10 seconds which was simulated. The battery had a shorter charging time when compared to the li-ion battery. The voltage seen in Figure 32 might indicate that the RC-parameters are wrong as the maximum and minimum voltages do not match the maximum and minimum voltage set out in the datasheet. As stated in Dell [7], the NiMH battery characteristics depend on the temperature. Without having the temperature development during the reaction, this might then influence the maximum and minimum voltage. Another explanation might be that the maximum and minimum voltage rated in the datasheet might not have been calculated at 1 A.

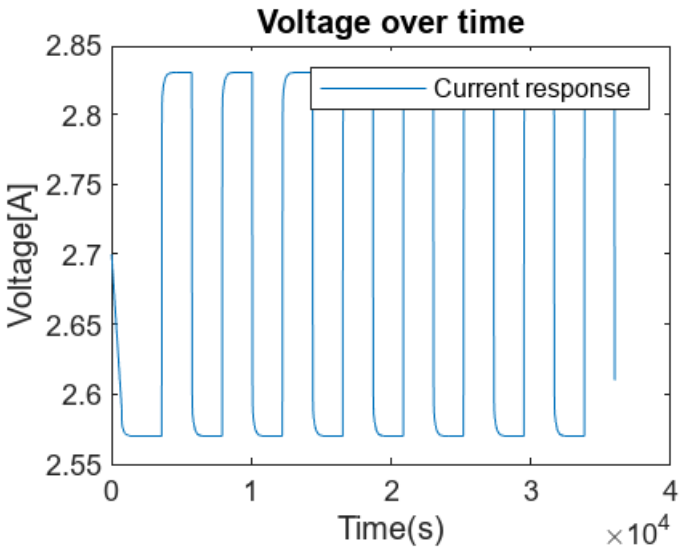


*Figure 32: Longrange simulation of NiMH battery voltage*

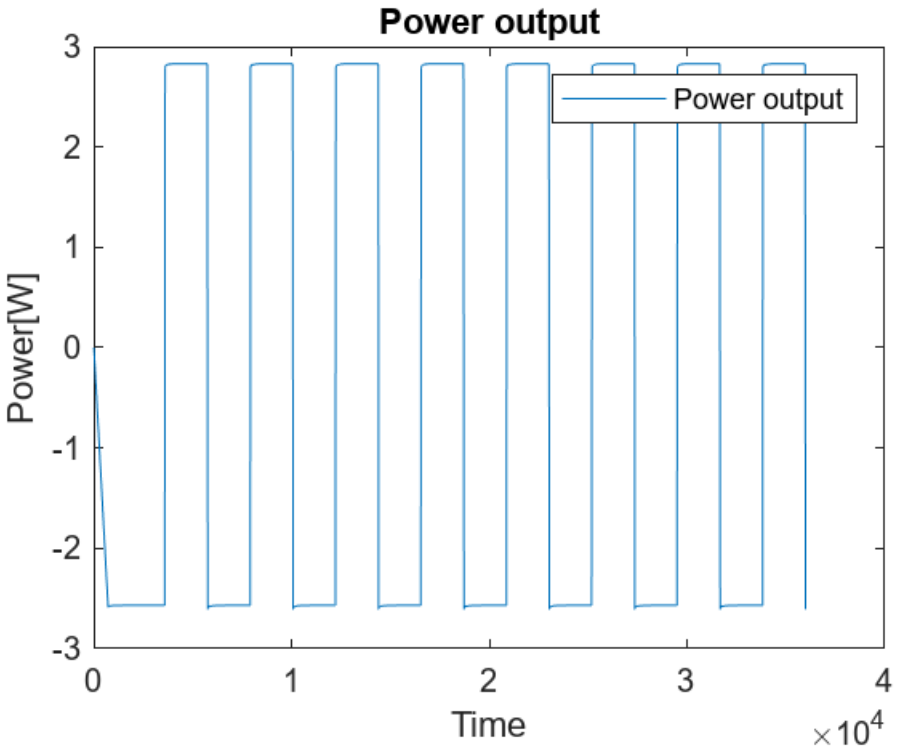


*Figure 33: Power output for NiMH battery during long range operations*

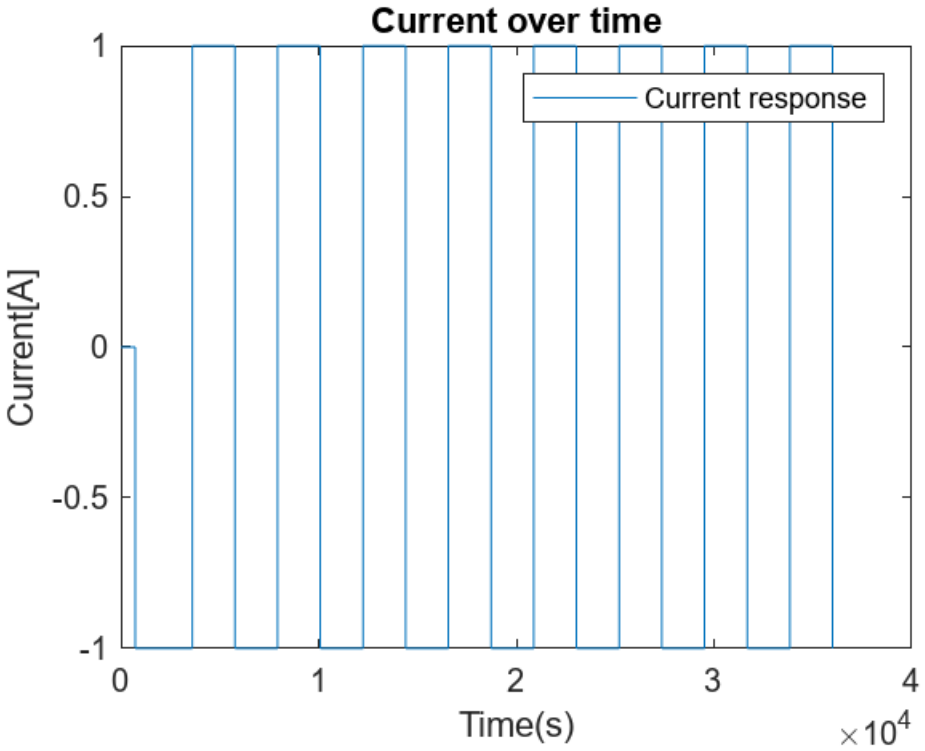


*Figure 34: Current over time during longrange operations NiMH battery*

## 4.6 Simulation of supercapacitors

### 4.6.1 Eaton 400F

The Eaton 400F supercapacitor showed a rapid decrease in the SOC over a short period of time. The SOC for the Eaton supercapacitor is shown in Figure 35. A similar cycle time can be seen in Blomquist et al. [57]. The voltage for the supercapacitor in Blomquist et al. [57] is however about 1.0 V. As seen in Table 1 this means that an aqueous electrolyte was used. The electrolyte used in the Eaton 400 F is made of aluminium meaning the voltage the Eaton achieves, is higher than the supercapacitor presented in Blomquist et al. [57] The Eaton supercapacitor stores enough charge to have a discharge cycle of about 40 seconds.

It was observed at about 70 seconds in the SOC begins to increase again. A similar behaviour was seen in L.E Helseth [47], and is mainly due to the time constants and the stabilization of the electrochemical system that make the voltage converge to the OCV after relaxing for a period. Equation 23 does not hit 0 during the simulation due to Vactual being close to zero, but not 0. This makes the SOC almost hitting 0. The for-loop only stops the simulation when the SOC is absolute zero, meaning that the simulation still runs for some time. For all practical purposes the SOC is nevertheless assumed to be 0 at t = 40 seconds in Equation 31. As the SOC for the battery allows the SOC reaching zero based on Equation 22, the simulation for the batteries stopped before being able to start the relaxation period and then start converging towards the OCV over time. If the SOC-loop was removed, the same phenomenon would also happen to the battery as both are  electrochemical in nature.

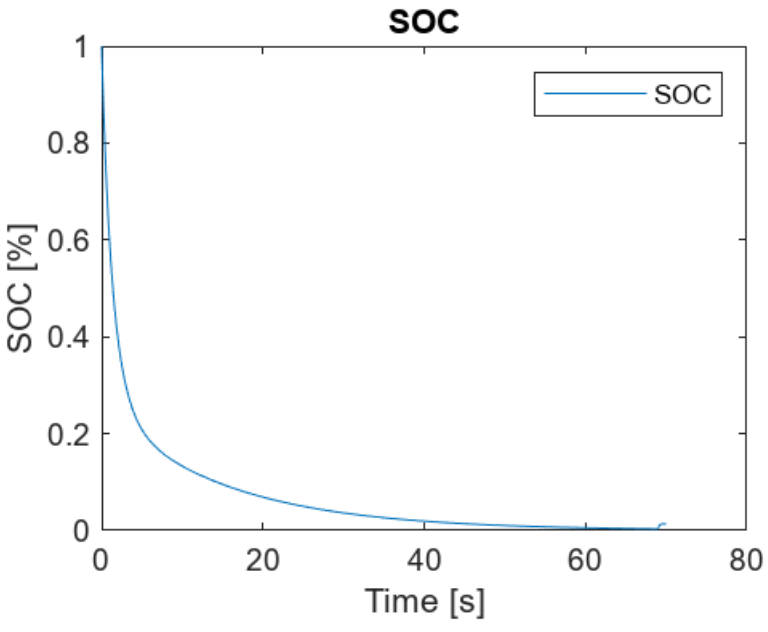

*Figure 35: SOC for the Eaton 400F supercapacitor*

The current and voltage for the Eaton were then plotted in Figure 36 and Figure 37. The power was plotted in Figure 38. The shape of the SOC is based on the voltage as seen in Equation 23. In Martellucci et al. [58] a 2.7 V supercapacitor simulated using an equivalent circuit model was able to give up to about 40 A for a pulse of 5 seconds. The supercapacitor simulated here reaches about 40 A and then gradually declines. There are however some differences between the models in this thesis and the model presented by Martellucci et al. [58]. The most relevant difference with for this  thesis was that the circuit model used in Martellucci et al. [58] was also combined with a li-ion battery. A similar surge of power was seen in Blomquist et al. [57] during discharging.

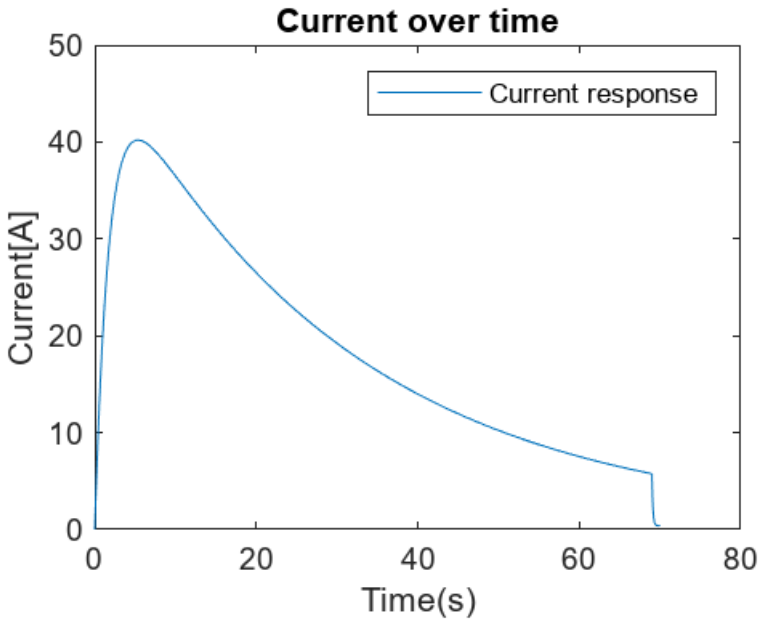


*Figure 36: Current over time for the Eaton 400F supercapacitor*

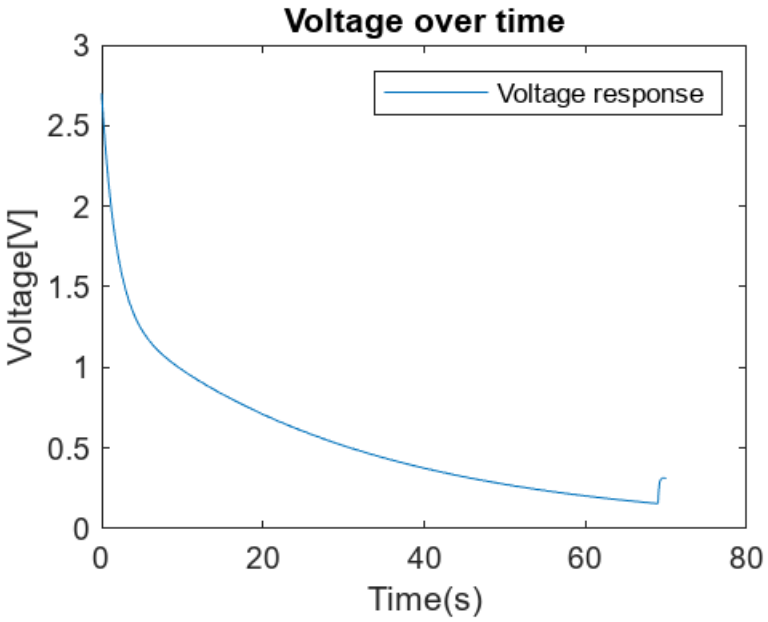


*Figure 37: Voltage over time for the Eaton 400F*

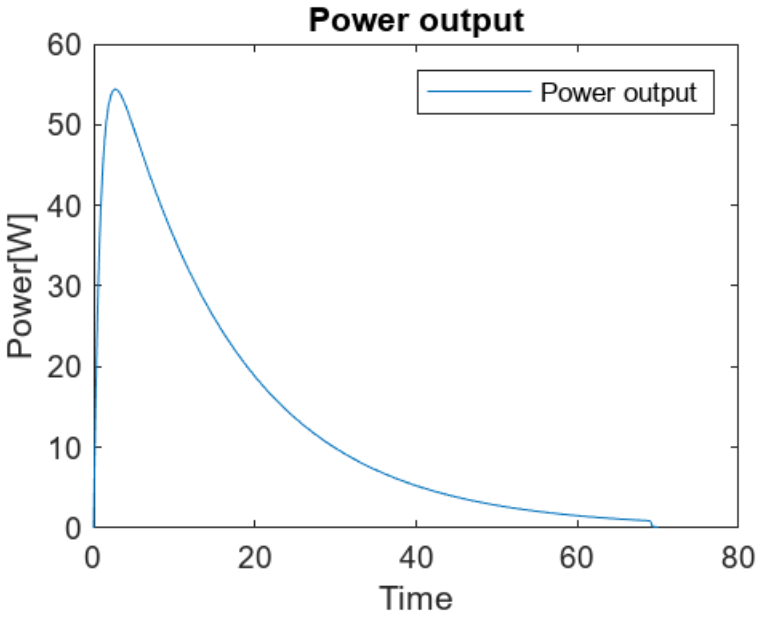


*Figure 38: Power over time for the Eaton 400F*

The voltage over current is shown in Figure 39. The plot during discharge takes the shape of the first half of a cyclic voltammetry. Similar shapes during discharge can be seen in Blomquist et al. [57] The plot might indicate that the supercapacitor provides a huge pulse of current, and then loses a lot of voltage even as the current through the supercapacitor is reduced. This is somewhat opposite of what was seen in both the batteries plotted in Figure 31 and Figure 23. In Køtz et al. [15] it is noted that supercapacitors during charging and discharging takes on

a more box-like shape when current over voltage is plotted for one full cycle. The maximum power seen was 54.1 W during discharge. It is noted that in the end of the cycle the SOC was increasing. This can also be seen in the voltage over current plot, and might be due to some side reactions and slow kinetics releasing a current, increasing the voltage and then the SOC.

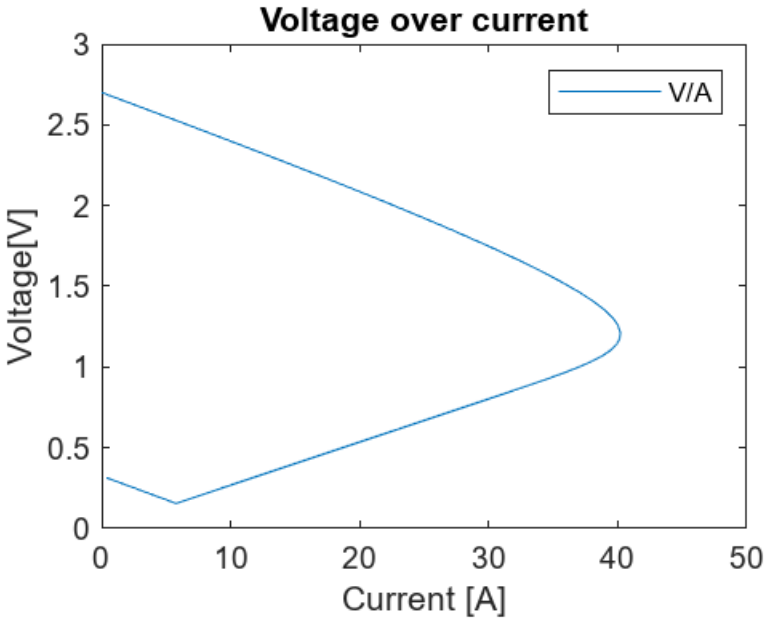


*Figure 39: Voltage over current for the Eaton 400F*

### 4.6.2 Eaton 400F longrange

A current of 4 A during charge and discharge was chosen for the Eaton supercapacitor. In Figure 41 and Figure 42 the voltage and power response are seen. Compared to the batteries the supercapacitors discharge all the way to zero, before then being recharged again. The shape is spikier then compared to the battery charging and discharging characteristics using a CC-CV block. The spikier shape means the supercapacitor gives a huge pulse and surge of power during a short amount of time, before it almost instantly is out of charge. The same behaviour for a supercapacitor cycle was seen in L. E Helseth [47] and Blomquist et al. [57] It is also important to notice that the supercapacitor was able to give 8 fully charging and discharging cycles in 10000 seconds, while the battery gave the same number of cycles during a longer time.

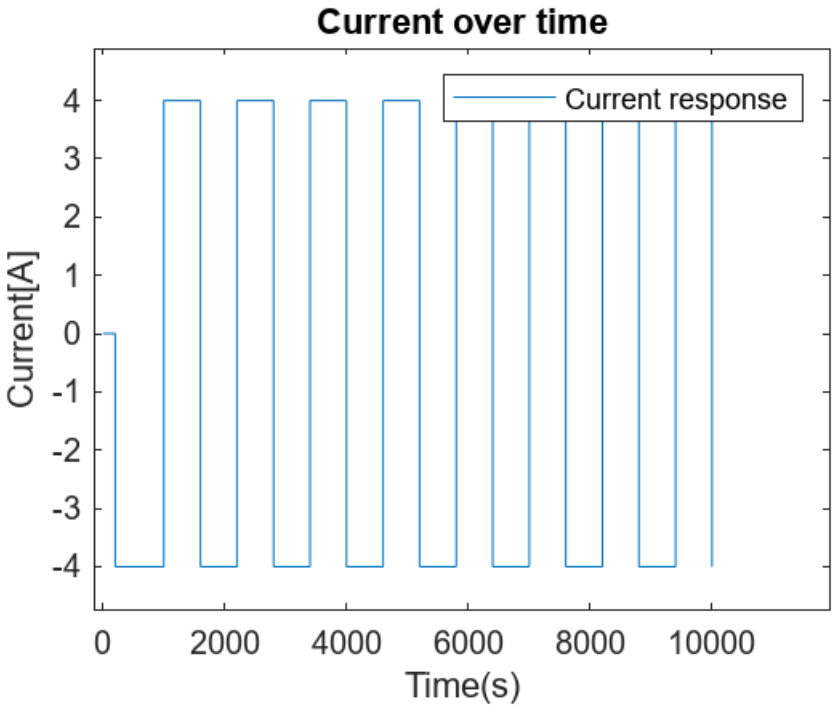


*Figure 40: Eaton 400F currents during long range operations*

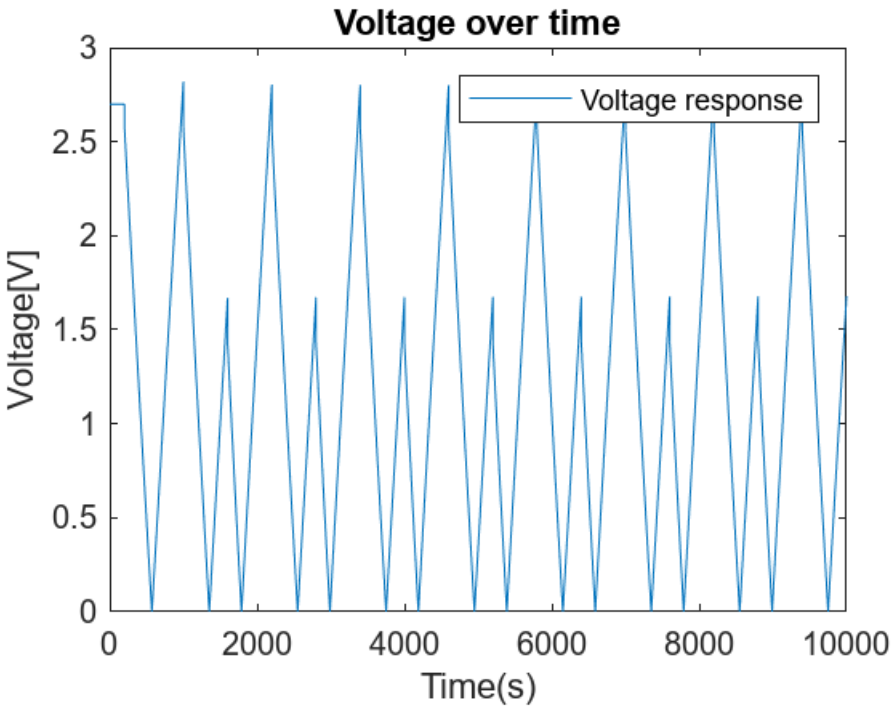


*Figure 41: Voltage over time for the Eaton 400F during longrange operation*

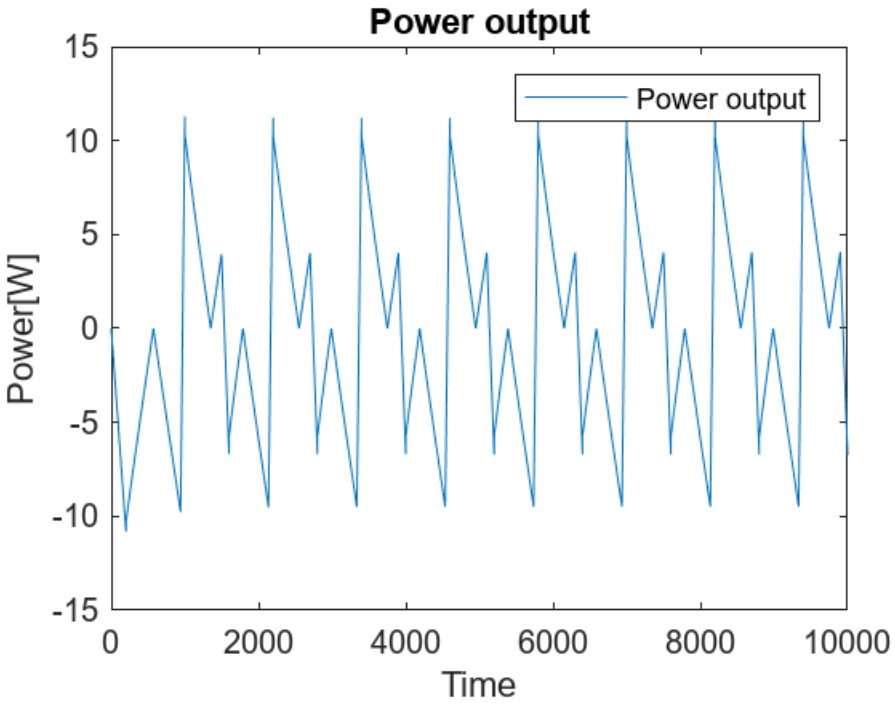


*Figure 42: Power output from the Eaton 400F during longrange operations*

### 4.6.3 Nichion 150F

For the Nichion 150 F Supercapacitor several similar tendencies were seen compared to the Eaton 400 F. The SOC was plotted in Figure 43. As the Nichion 150F has less capacitance when compared to the Eaton 400F, it has a shorter discharge time when the same load is applied. The current and power output seen in Figure 44 and Figure 46 show that both the power and current that the supercapacitor gave were less than the Eaton 400F. The voltage was plotted in Figure 45. The maximum power the Nichion was able to give was about 42 W, while the discharge cycle only lasted 20 seconds. For the Nichion supercapacitor no rise of voltage was observed after the load was disconnected as seen in Figure 47. This might be due to the Nichion needing more time for the voltage to start converging towards the OCV. As there was no increase of voltage, the voltage over current plot indicates no increase of voltage when the current is reduced towards the end of the cycle. This might be due to how the different RC-parameters, and the relation between the parameters, affect the voltage of the supercapacitor.

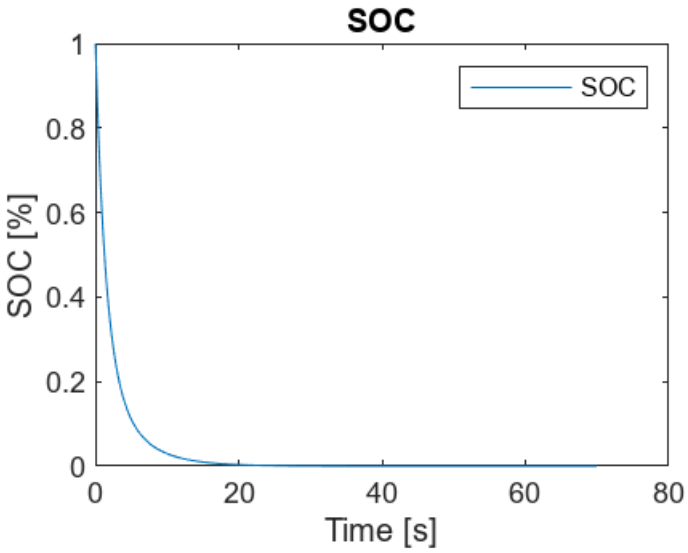


*Figure 43: Nichion 150F SOC*

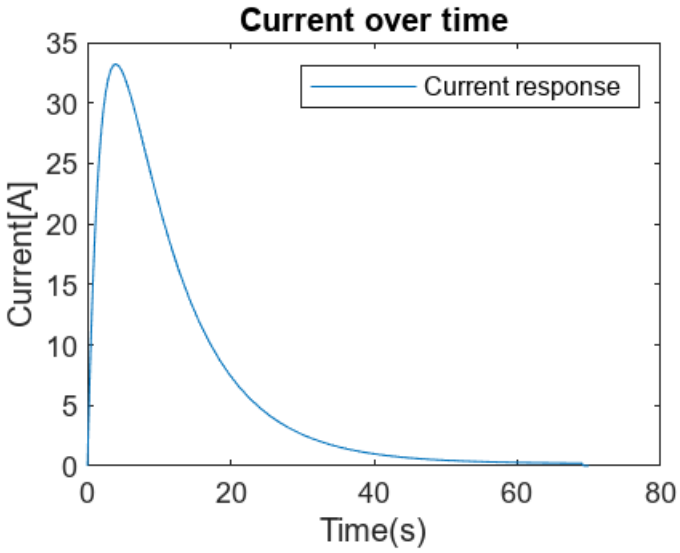


*Figure 44: Current over time Nichion 150F*

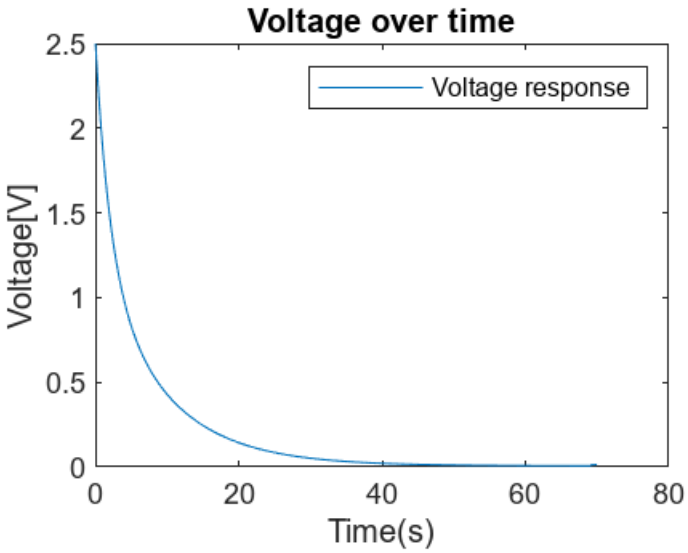

*Figure 45: Voltage over time Nichion 150F*

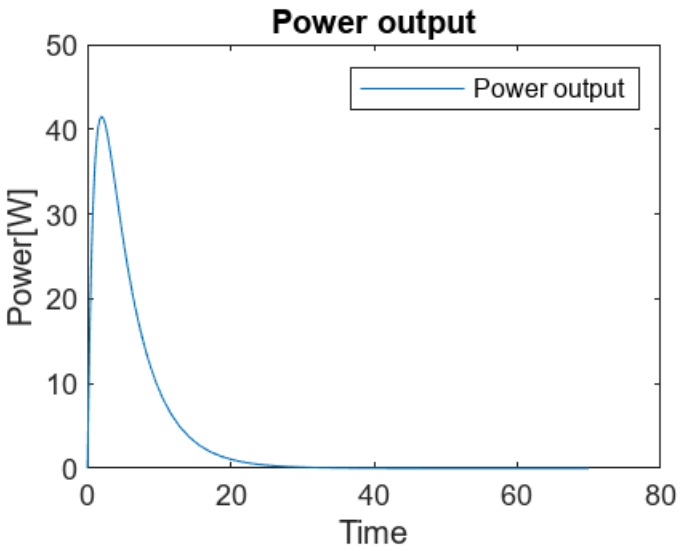


*Figure 46: Power output Nichion 150F*

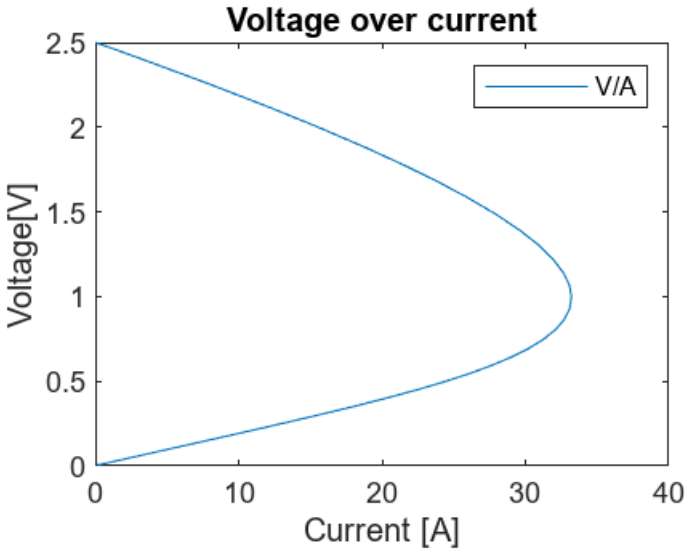


*Figure 47: Voltage over current Nichion 150F*

### 4.6.4 Nichion Longrange

For the Nichion supercapacitor a lower current was tested. The main difference seen here was that when using a lower current, the Nichion supercapacitor was able to have 8.5 full cycles during the simulation of 10000 seconds. Due to the Nichion having a lower rated voltage and using a lower current, the power output during the long-range cycles was less than that for the Eaton supercapacitor. The power, current, and voltage is plotted in Figure 48, Figure 49 and Figure 50.

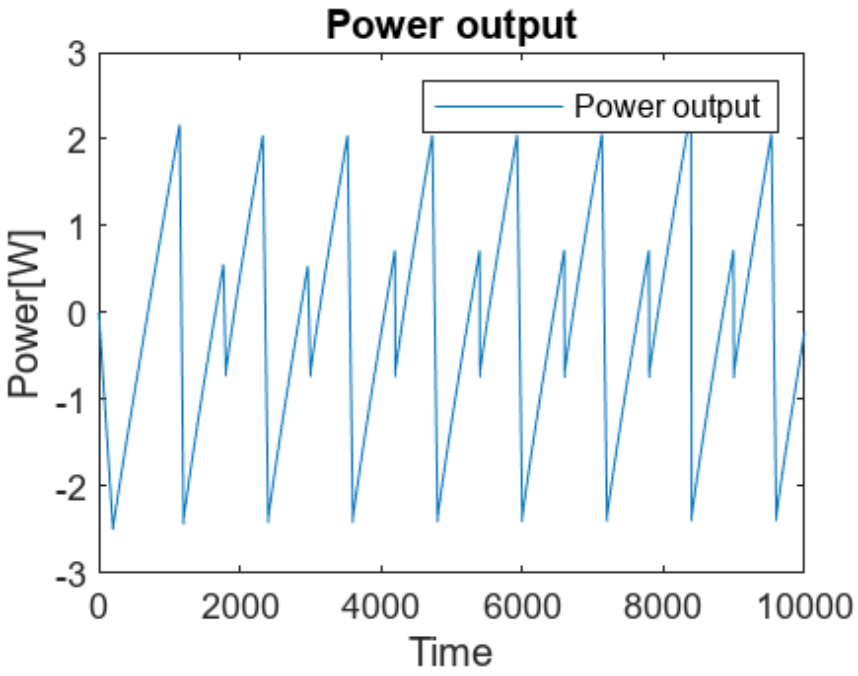


*Figure 48: Power output Nichion 150F*

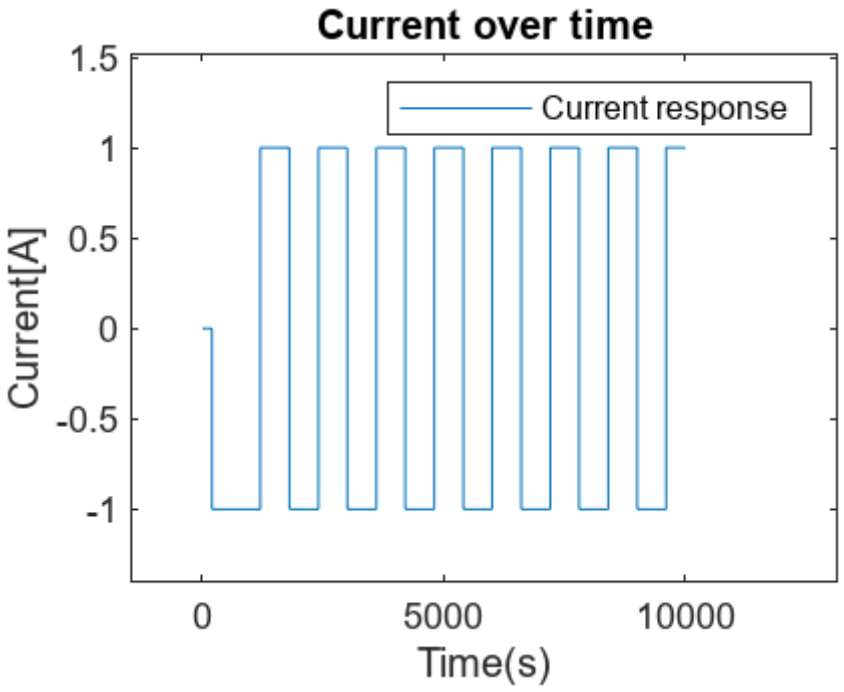


*Figure 49: Current over time Nichion 150F*

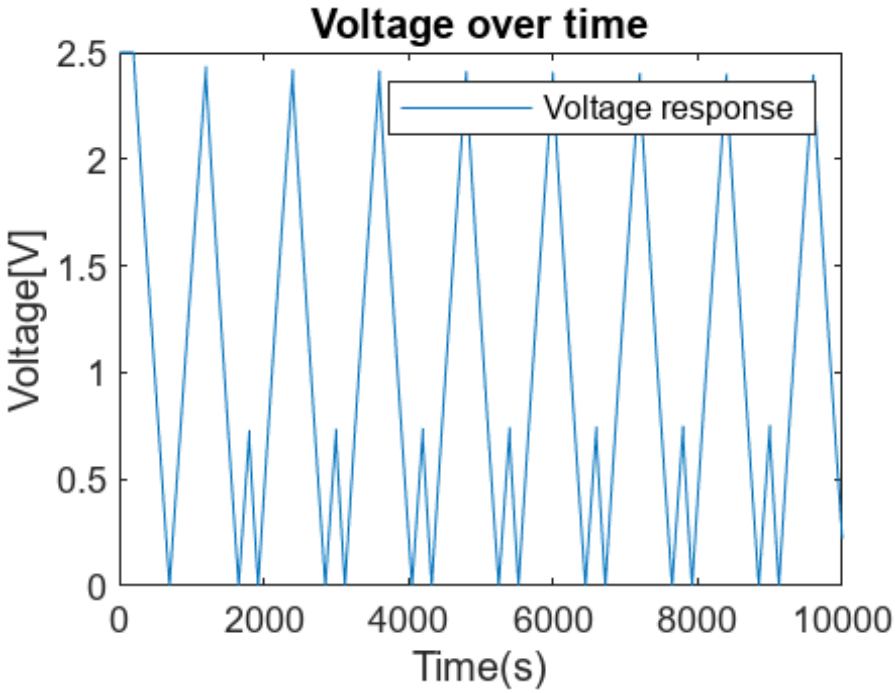


*Figure 50: Voltage over time Nichion 150F*

## 4.7 State of health

The SOH was then assumed to linearly decline for both the batteries and supercapacitors. Using Equation 24 and the results from the simulations, a basis was decided for the current and power flowing when the energy storage devices were at their peak. This was used as a starting point for the calculation of the SOH over time. It was assumed that the resistance over time was increasing by 0.0001 ohm per cycle. In order to consider some of the temperature dependencies brought up by Dell [7], it was assumed that the resistance was increasing faster for the NiMH battery. To test the estimated lifetime the constant current constant voltage was tested. All assumptions and results of using Equation 31 are shown in Table 12 below.

*Table 12: SOH estimation for the energy storage devices*

| Device | Resistance increases 1 | Max power | Current (discharge) | Cycles | Discharge lifetime |
|---|---|---|---|---|---|
| Eaton 400F | 0.0001 | 15 W | 4 A | 1750 | 19.44 hrs |
| Nichion 150F | 0.0001 | 2 W | 1 A | 4001 | 22.22 hrs |
| Li-ion battery | 0.0001 | 10 W | 5.6 A | 639 | 115.375 hrs |
| NiMH battery | 0.001 | 2.6 W | 1 A | 521 | 115.77 hrs |

By assuming that the SOH declines linearly, the supercapacitors are better in terms of estimated cycle life. As the current also plays a role in Equation 31, the lower current devices are also able to give more cycles. In Køtz et al. [15] it is stated that supercapacitors in general have a longer cycle life than batteries. Based on the results of the SOH estimation, this can clearly be seen. The discharge time shows how much useful discharge time the storage device can give. This is based on the SOC plots for the supercapacitors and batteries. As the supercapacitors in general had shorter discharge times, the useful discharge lifetime will be less than that for the batteries. While the li-ion battery had a longer cycle-lifetime than that of the NiMH battery, the discharge lifetime was about the same due to the NiMH battery having a longer cycle time.

Due to the different polarizations as well as a reduction in the area where ions can move on the anode and the cathode, the assumption of degradation being linear is not the most accurate [26] [42]. The original plan of the thesis was to increase the resistance in the Simulink models to see how the change of resistance would affect the circuit dynamics modelled. Due

to the models crashing and time constraints, it was decided that assuming a linear cycle degradation was enough to roughly estimate the expected lifetime.

## 4.8 Suggestions for future work

Based on the simulations in this thesis it is evident that further research can be carried out. Such research can be based directly on some of the results of this thesis. This can either be done as research papers, or as a new thesis. Suggestions for future research is listed below:

- Investigate how temperature affects the supercapacitor and battery dynamics used in this thesis and then verify how the SOH is affected
- Perform laboratory tests of the specific batteries and supercapacitors to verify the RC parameters used in the equivalent circuit models while also adding heat transfer dynamics
- Expand the equivalent circuit models to include heat transfer and effect of temperature
- Combine the supercapacitor and battery model as the literature study mentioned, and observe how that affects the cycle life, SOH and SOC
- Construct a model of an EV in Simulink, and build battery/supercapacitor packs based on the models proposed in this thesis
- Do the SOH calculations based on actual RC-parameters with heat transfer and real-life load conditions to find an improved model for degradation for the different batteries

## 4.9 Final discussion

The simulations confirm what has been stated in the literature. As Yang et al. [29] showed that supercapacitors can be used for buses, the simulations of both the Nichion and Eaton supercapacitor support the findings of needing to charge for every trip. The power surge is quite large as seen in Figure 38 and Figure 48, while the supercapacitors are discharged rapidly.

A number of the issues with renewables in the grid were brought up by Durganjali et al. [4], and Knut Hofstad [6]. The grid needs constant loads and systems that can ramp up power into the grid to remain stable. The slow-paced system needs to be able to deliver a constant power/load over time, while a fast-paced system is also needed to handle the power surges [14]. Durganjali et al. [4] concluded that batteries were excellent for the slow-paced system while supercapacitors were exceptional for the fast surge system. This is also supported by the simulations done here.

If a high power over time is needed the simulations show that the best device is the lithium battery. If a small but constant power over time is needed with a more stable voltage source, the NiMH battery is more suited. If a system requires a large surge of current and power over a short amount of time, then both supercapacitors can be used. The main difference between the two different supercapacitors was how long a large surge of power could be delivered. Which supercapacitor is needed will therefore mainly depend on how much power is needed and how long the power is required for the application being used.

Based on the SOH estimation the batteries had a shorter lifetime in terms of the number of cycles that they could be used. Batteries had the longest expected lifetime when considering the number of hours the devices could be used. This might be because the batteries had a longer cycle time when compared to the supercapacitors. In Powade et al. [27] the number of cycles a battery pack connected to a varying load could perform 2440 cycles [27]. When combining the batteries with supercapacitors the estimated amounts of cycles rose to 2660 [27]. A varying load with different depths of discharge might affect the degradation and the SOH, and then the expected lifetime. Compared to Powade et al. [27] the values calculated here might indicate the load used in this thesis being more extreme. This might imply the load being used in this thesis does not accurately represent an average load situation

# 5 Conclusions

The conclusion of this thesis is that batteries are superior to supercapacitors when it comes to load requirements over time. Supercapacitors, however, are superior to batteries when it comes to supplying short term pulses. The literature suggests batteries and supercapacitors should be used for different applications like electric vehicles, medical equipment and the power grid based on the specific requirements. The literature highlights the main issue of batteries to having a long charging time, while supercapacitors have a fast cycle time. Simulations of batteries and supercapacitors confirmed this. To mitigate these issues the literature recommends placing supercapacitors and batteries in a combined system. The SOH calculations show that the supercapacitors can give more cycles, and batteries can give more discharge hours. It is recommended to conduct further research into how a combination of batteries and supercapacitors could perform in different types of actual applications.

# 6 References


[1] The united nations, «United Nations,» United Nations, 16 Oktober 2022. [Internett]. Available: https://sdgs.un.org/goals/goal13. [Funnet 26 April 2023].

[2] The European Commission, «REPowerEU: A plan to rapidly reduce dependence on Russian fossil fuels and fast forward the green transition,» The European Union, Brussels, 2022.

[3] United Nations, «Paris agreement,» i *United Nations*, Paris, 2015.

[4] C. S. Durganjali, V. Chawla, H. Raghavan og S. Radhika, «Design, development, and techno-economic analysis of extreme fast charging topologies using Super Capacitor and Li-Ion Battery combinations,» *Journal of Energy Storage,* 10 December 2022.

[5] Norges vassdrag og energi direktorat, «Elektrifiseringstiltak i Norge,» NVE, Oslo, 2020.

[6] K. Hofstad, «Store norske leksikon,» SNL, 22 Januar 2023. [Internett]. Available: http://snl.no/grunnlast. [Funnet 3 Februar 2023].

[7] R. Dell og D. RAND, Understanding batteries, Cambridge: The Royal Society of Chemistry, 2001.

[8] E. Thomas og R. Phillip, Thermodynamics, Statistical Thermodynamics, and Kinetics, Washington: Pearson Educational, 2021.

[9] V. S. Bagotsky, Fundamentals of electrochemistry 2nd edition, Moscow: Wiley and sons, 2006.

[10] B. Claus og E. Richard, Borgnakke's fundamentals of thermodynamics, Michigan: John WIley and Sons, 2017.

[11] S. B. Lawrence og A. H. Thomas, Chemistry for engineering students, Texas: Cengage learning , 2015.

[12] P. Jung-Ki, Principles and applications of Lithium Secondary Batteries, Weinheim: Wiley-VCH, 2012.

[13] H. Wei, K. Marcus, L. Xing, D. Mark, L. Dacheng og W. Jihon, «Technologies and economics of electric energy storages in power systems: Review and perspective,» *Advances in Applied Energy,* 19 November 2019.

[14] B. Alberto, S. M. Idoia, P. Sanchis og A. Ursúa, «Lithium-ion batteries as distributed energy storage systems for microgrids,» i *Distributed Energy Resources in Microgrids*, Academic Press, 2019, pp. 143-183.

[15] R. Køtz og M. Carlen, «Principles and applications of electrochemical capacitors,» *Electrochimica Acta 45,* p. 2483–2498, 1 Januar 2000.

[16] S. M og N. S, Elements of Electromagnetics - 7th edition, Oxford : Oxford University Press Inc, 2021.

[17] A. Afif, S. M. Rahman, A. Tasfiah, J. Zaini, M. A. Islan og A. K. Azad, «Advanced materials and technologies for hybrid supercapacitors for energy storage – A review,» *Journal of Energy storage,* 19 October 2019.

[18] J. Yu, N. Fu, J. Zhao, R. Liu, F. Li, Y. Du og Z. Yang, «High Specific Capacitance Electrode Material for Supercapacitors,» *ACS Omega,* pp. 15904-15911, 14 April 2019.

[19] T. Wells, «Determining the voltage range of a carbon based super capacitor,» Examensarbeten i Energiteknik, Berlin, 2014.

[20] «Metal oxide-based supercapacitors: progress and,» *Cuihua An;ab Yan Zhang;a Huinan Guo;a Yijing Wang,* 30 October 2019.

[21] K. Fong, T. Wang og S. K. Smoukov, «Multidimensional performance optimization of conducting polymer-based,» *Sustainable energy and fuels,* nr. 9, pp. 1857-1874, 2017.

[22] Elna, «Elna,» 2021. [Internett]. Available: www.elna.co.jp/en/product/caluclation_double_layer/?fbclid=IwAR3wMBKewEOdbA0_j0rs0Q-FbQqHr-VMYWSbpyznFYn-vDSfM8kTVXa8Uk0. [Funnet 13 April 2023].

[23] J.-K. Yong og D. C. Byung, «Energy consumption optimization for the electric vehicle routing problem with state-of-charge-dependent discharging rates,» *Journal of cleaner production,* 20 Januar 2023.

[24] P. Ma, J. Shu, X. Zhao, Y. Cao, L. Wang, G. Chen, J. Wu og Y. Mi, «The CrBr3 monolayer: Two dimension sodium ion battery anode material to characterize state-of-charge by magnetism,» *Applied Surface science,* pp. 1570-1574, 30 Juni 2023.

[25] «Eaton - Powering Business World wide,» Eaton, 1 Januar 2023. [Internett]. Available: www.eaton.com/us/en-us/products/electronic-components/faq/supercapacitor-modules-frequently-asked-questions.html. [Funnet 18 April 2023].

[26] M. Murnane og A. Ghazel, «A Closer Look at State of Charge and State of Health estimations for batteries,» Analog devices, Berlin, 2017.

[27] P. Rajat og B. Yogesh, «Design of semi-actively controlled battery-supercapacitor hybrid energy storage system» *Materials Today: Proceedings,* pp. 1503-1509, 1 Januar 2023.

[28] L. Guo, H. Pan og W. Hong, «Development of supercapacitor hybrid electric vehicle,» *Journal of energy storage,* 15 August 2023.

[29] H. Y. Li, L. Q. E., Z. D. Gong, X. G. X. J. H. Zhang og X. L. Miao, «Supercapacitor powertrain system used in shanghai expo 2010 for public transportation city bus and its popularization,» *China Acad,* 2011.

[30] M. Petit, C. Elisa og B. Julien, «A simplified electrochemical model for modelling Li-ion batteries comprising blend and bidispersed electrodes for high power applications,» *Journal of power sources,* 15 December 2020.

[31] J. Marijn R og Boud, «Which battery model to use?,» 16 May 2009. [Internett]. Available: https://ris.utwente.nl/ws/portalfiles/portal/6728809/IET-final-beta.pdf. [Funnet 18 April 2023].

[32] M. Martin, T. B. Norman, R. Peter M, H. Markus W og J. Tubke, «Comprehensive determination of heat generatic thermal modelling of a hybrid capacitor,» *Journal of power sources,* 30 September 2019.

[33] H. J.I, G.-A. J.F, R. Escobar-Jiménez og A.-M. L.-L. V.M, «Classical and fractional-order modeling of equivalent electrical circuits for super capacitors and batteries,» *Microelectronics Journal,* pp. 109-128, 1 March 2019.

[34] B. Nikhil og F. Huazhen, «BattX: An equivalent circuit model for lithium-ion batteries over broad current ranges,» *Applied Energy,* 1 June 2023.

[35] S. Stefan, «Parameterization of Equivalent Circuit Models for High Power Lithium-Ion,» Chalmers University of Technology, Gothenburg, 2016.

[36] C. Bin-Hao, P.-T. Chen, L. Y. Yen og L. Hua-Sheng, «Establishment of second-order equivalent circuit model for bidirectional voltage regulator converter: 48 V-aluminum-ion battery pack,» *Energy reports,* pp. 2629-2637, 1 December 2023.

[37] C. Fan, K. O'Regan, L. Li, M. D. Higgins, E. Kendrick og W. D. Widanage, «Data-driven identification of lithium-ion batteries: A nonlinear equivalent circuit model with diffusion dynamics,» *Applied Energy,* 1 September 2022.

[38] B. Robert L og N. Louis, Electronic Devices and Circuit Theory, London: Pearson Education Limited, 2014.

[39] R. R. Thakkar, Management and Applications of Energy Storage Devices, Istanbul: Nişantaşı university, 2021.

[40] T. Ning, W. Yebin, C. Jian og H. Fang, «On Parameter Identification of an Equivalent Circuit Model for Lithium-Ion batteries,»

i *2017 IEEE Conference on Control Technology and Applications (CCTA)*, Kohala Coast, Hawai'i, 2017.

[41] D. G. L. Plett, «UCCS: University of Colorado Springs,» 1 Januar 2018. [Internett]. Available: http://mocha-java.uccs.edu/ECE5710/index.html. [Funnet 21 April 2023].

[42] J. Samppa, H. Ari, H. Jari og P. Mikko, «State of health estimation of cycle aged large format lithium-ion cells based on partial charging,» *Journal of energy storage,* 17 February 2022.

[43] Z. Cheng, A. Walid, D. Quang, A. Pedro og M. James, «Online estimation of battery equivalent circuit model parameters and state of charge using decoupled least squares technique,» *Energy,* pp. 678-699, 1 January 2018.

[44] Samsung, «samsung.com,» 1 Januar 2023. [Internett]. Available: no.rs-online.com/web/p/speciality-size-rechargeable-batteries/8801551?cm_mmc=NO-PLA-DS3A-_-google-_-CSS_NO_NO_Batteries_%26_Chargers_Whoop-_-(NO:Whoop!)+Speciality+Size+Rechargeable+Batteries-_-8801551&matchtype=&pla-339269539139&gclid=CjwKCAjw6Ii. [Funnet 1 May 2023].

[45] K. Norian, «Equivalent circuit components of nickel–metal hydride battery at different states of charge,» *Journal of power sources,* pp. 7812-7815, 15 September 2011.

[46] GlobTek, «digikey.no,» 1 January 2023. [Internett]. Available: www.digikey.no/en/products/detail/globtek-inc/BM2000C1450AA2S1PATP/10187624?gad=1&gclid=CjwKCAjw6IiiBhAOEiwALNqncd08riaZCuFcbrEezBoZsw3A3aUWtjePDpPXBj-fFayqtHK_Y4kqZxoCvpYQAvD_BwE&s=N4IgjCBcoCxgTFUBjKAzAhgGwM4FMAaEAeygG0QBmADgAZaB2CAXSIAcAXKEAZQ4C. [Funnet 1 May 2023].

[47] L. Helseth, «Modelling supercapacitors using a dynamic equivalent circuit with a distribution of relaxation times,» *Journal of energy storage,* 1 October 2019.

[48] L. Khaled og C. Antonio J. Marques, «A review of supercapacitors modeling, SoH, and SoE,» *International journal of energy research,* p. 18424–18440, 20 June 2021.

[49] R. Faranda, «A new parameters identification procedure for simplified double layer,» *Electric Power Systems Research,* pp. 363-373, 22 October 2009.

[50] Nichion, «RS,» 1 January 2023. [Internett]. Available: https://no.rs-online.com/web/p/supercapacitors/7149010?cm_mmc=NO-PLA-DS3A-_-google-_-CSS_NO_NO_Passive_Components_Whoop-_-(NO:Whoop!)+Supercapacitors-_-7149010&matchtype=&aud-772940708119:pla-338368499704&gclid=CjwKCAjw6IiiBhAOEiwALNqncZCKX6K75tFIXbg20rwM. [Funnet 1 May 2023].

[51] Eaton, «RS,» 1 January 2023. [Internett]. Available: no.rs-online.com/web/p/supercapacitors/

1699488?cm_mmc=NO-PLA-DS3A-_-google-_-CSS_NO_NO_Passive_Components_Whoop-_-(NO:Whoop!)+Supercapacitors-_-1699488&matchtype=&pla-301057795080&gclid=CjwKCAjw6IiiBhAOEiwALNqncXvVNrwBGYtYwVnbzAAtyOdrK0g8Gf4dKRgVE. [Funnet 1 May 2023].

[52] Battery Design, «Battery Design,» Battery Design, 1 January 2023. [Internett]. Available: www.batterydesign.net/ lifetime/?fbclid=IwAR0giRFdWLhk26Bpc79x5sJvdJf5cVglHaxBWiG2xVu8qwkUAXwFCjglu-Q. [Funnet 1 May 2023].

[53] S. Pai og M. R. Sindhu, «Intelligent driving range predictor for green transport,» i *IOP Conference Series: Materials Science and Engineering*, 2019.

[54] A. M. Casanova, A. S. Bray, T. A. Powers og A. J. Nimunkar, «Battery Power Comparison to Charge Medical Devices in developing countries,» i *International Conference of the IEEE Engineering in Medicine and Biology Society*, 2009.

[55] R. M. Shadman, D. D.L, M. Baghalha, K. M og N. P.H.L, «Adaptive thermal modeling of Li-ion batteries,» *Electrochimica Acta,* pp. 183-195, 28 March 2013.

[56] U. Krishnamoorthy, P. G. Ayyavu, H. Panchal, D. Shanmugam, S. Balasubramani, A. J. Al-rubaie, A. Al-khaykan, A. D. Oza, S. Hembrom, T. Patel, P. Vizureanu og D.-P. Burduhos-Nergis, «Efficient Battery Models for Performance Studies-Lithium Ion and Nickel Metal Hydride battery,» MDPI, KArur, 2023.

[57] N. Blomquist, T. Wells, B. Andres, J. Bäckström, S. Forsberg og H. Olin, «Metal-free supercapacitor with aqueous electrolyte and low cost carbon materials,» Scientific reports, Gothenbourg, 2017.

[58] L. Martellucci, M. Dell'Aria og R. Capata, «Experimental Analysis and Simulation of Mixed Storage with Lithium-Ion Batteries and Supercapacitors for a PHEV,» *Energies,* 4 May 2023.

[59] L. Yongchung og L. Shuo, «Research on bi-directional four-port converter of solar electric vehicle,» i *3rd International Conference on Power, Energy and Electrical Engineering (PEEE 2022)* , Barcelona, 2022.

[60] I. . Progressive Dynamics, «How Lead Acid Batteries Work: Battery Basics,» , . [Internett]. Available: http://www.progressivedyn.com/battery_basics.html. [Funnet 13 5 2023].

## Appendix A: Li-ion simulation Case 2

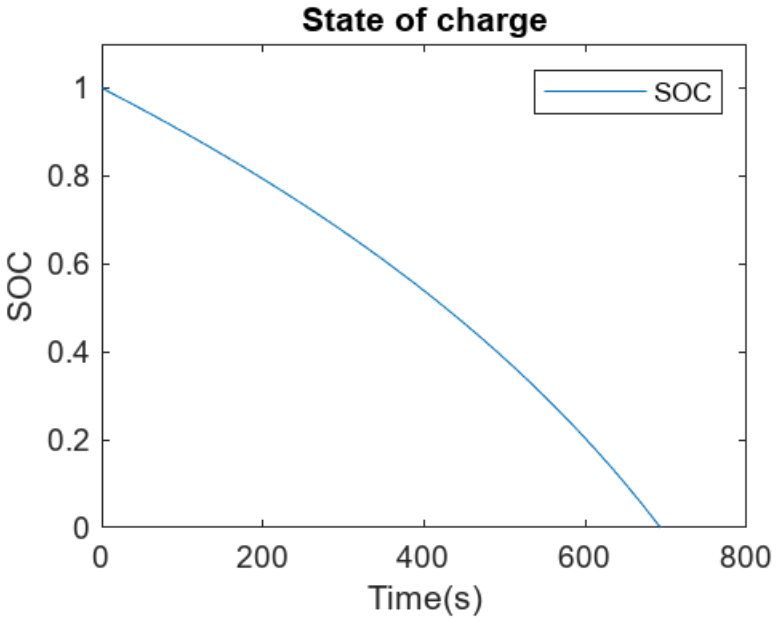


*SOC for the lithium battery(case 2)*

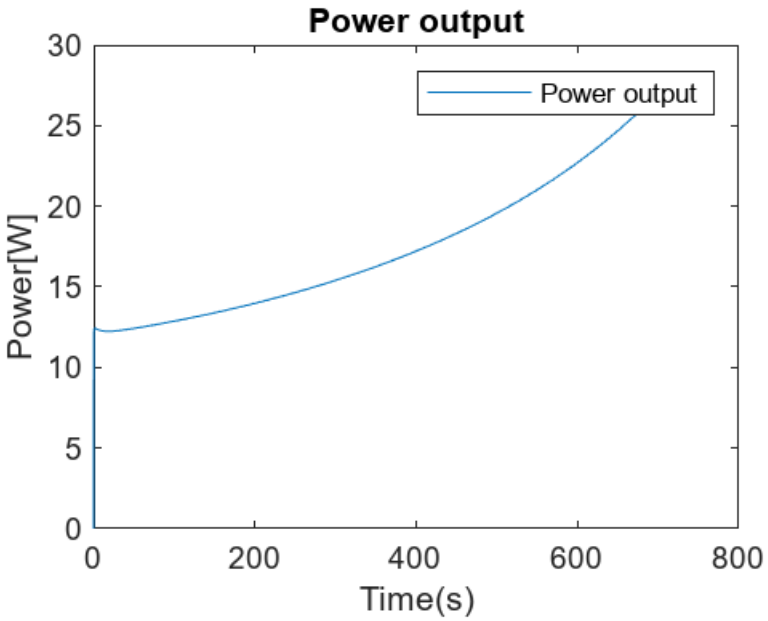


*Power output for the lithium battery (case 2)*

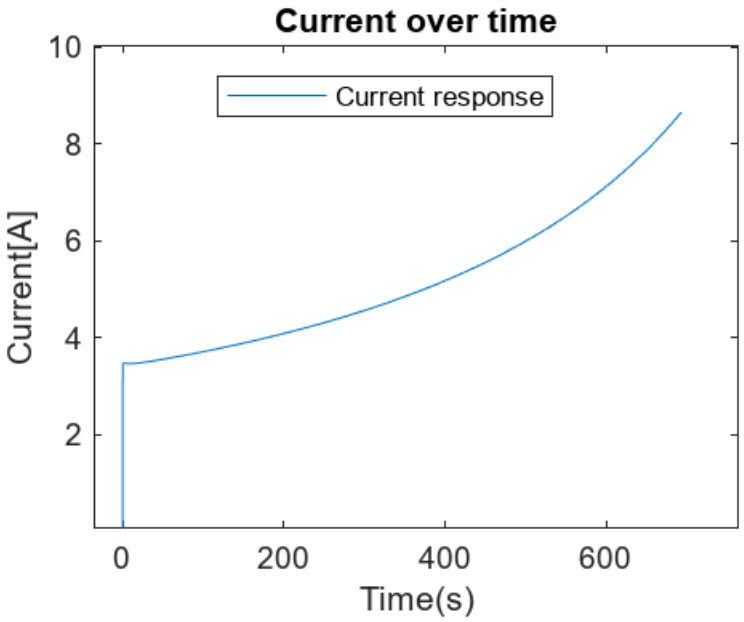


*Current over time for the Lithium battery(case2)*

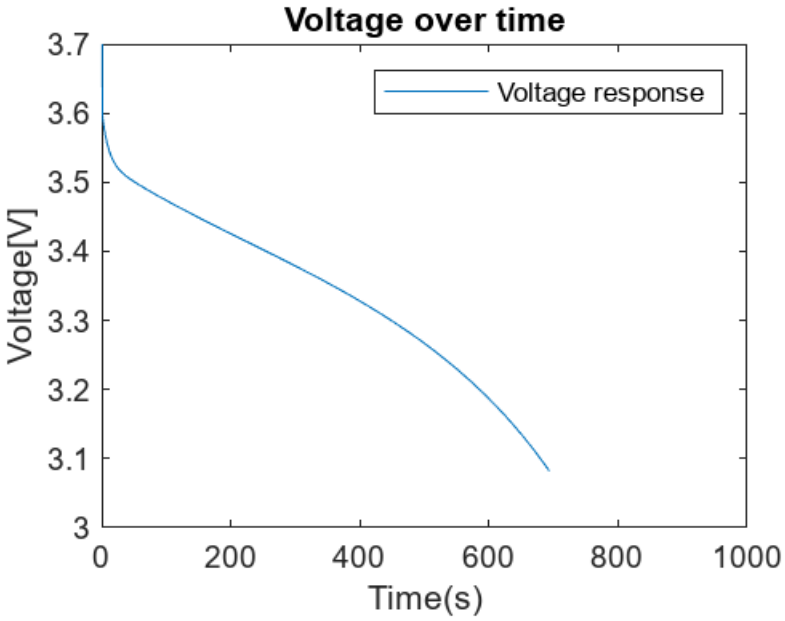


*Voltage over time for the lithium battery (case2)*

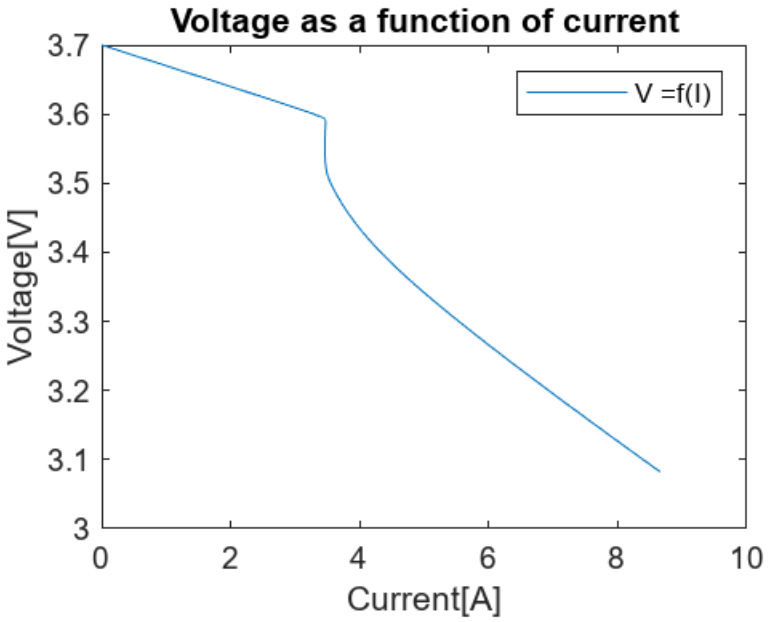


*Voltage as a function of current lithium battery (case 2)*

## Appendix B: NiMH battery simulation case 2

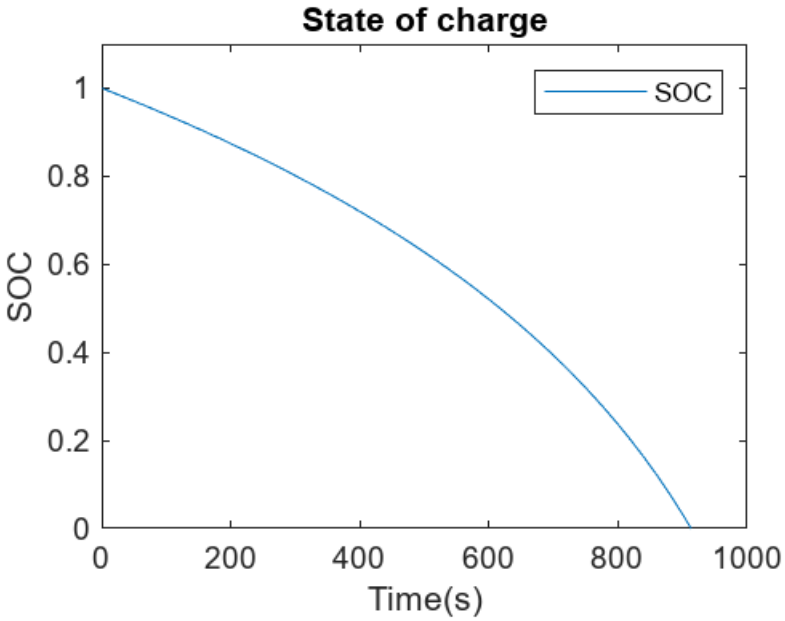


*SOC over time NiMH battery(case 2)*

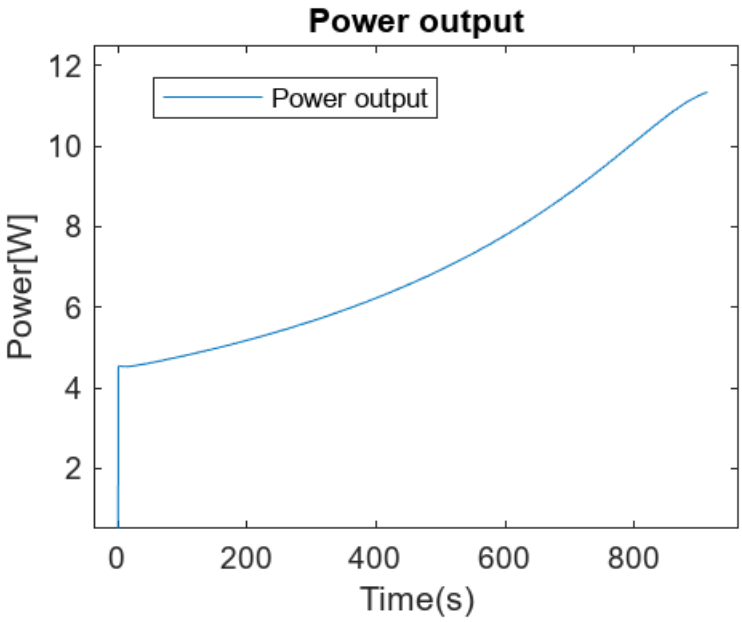


*Power output NiMH battery (case 2)*

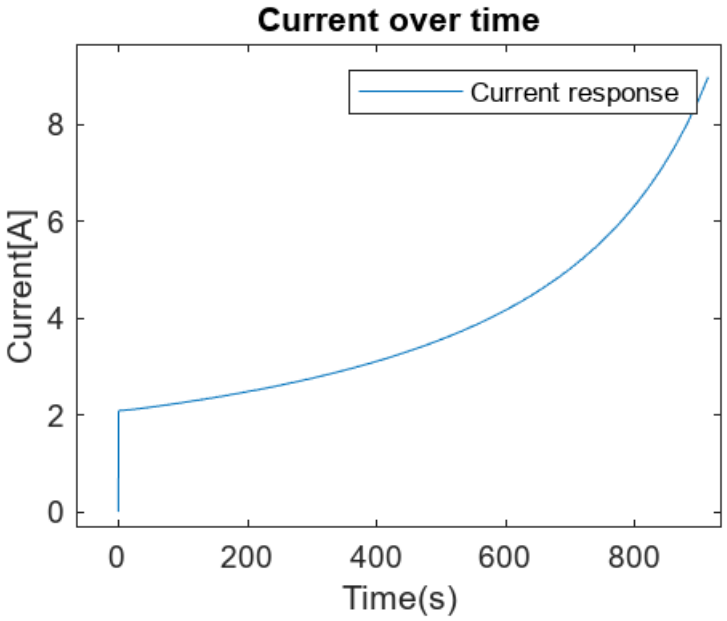


*Current over time NiMH (case2)*

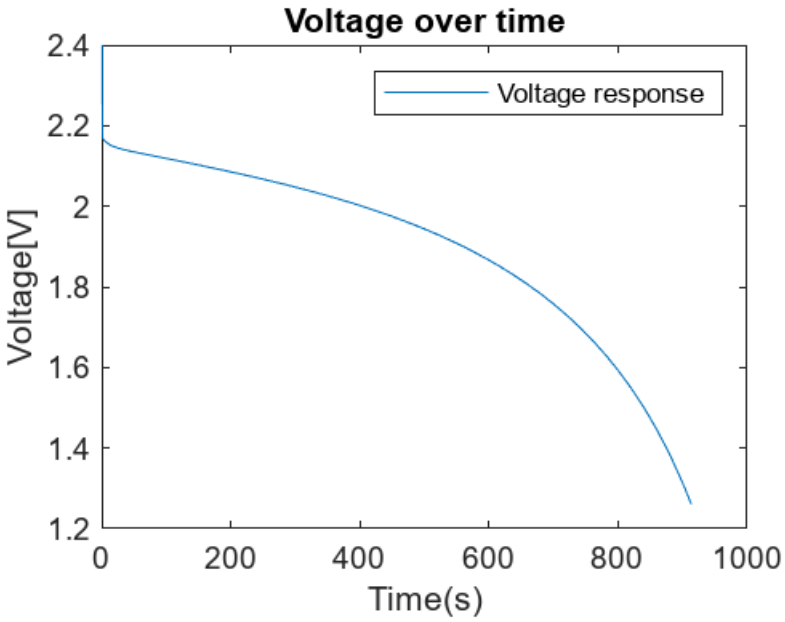


*Voltage over time NiMH (case 2)*

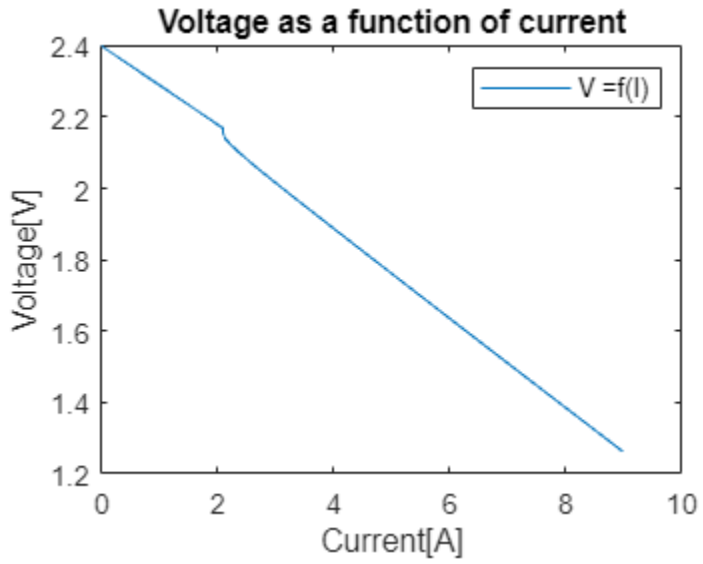


*Voltage as a function of current NiMH(case 2)*

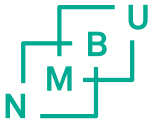


**Norges miljø- og biovitenskapelige universitet**
Noregs miljø- og biovitskapelege universitet
Norwegian University of Life Sciences

Postboks 5003
NO-1432 Ås
Norway